



Abbott Laboratories

Neuromodulation

6901 Preston Rd.

Plano, TX 75024

800-727-7846

FCC SAR and RF Exposure Evaluation Report

For

Abbott Laboratories

Neuromodulation 6901 Preston Rd. Plano, TX 75024

MODEL: 16000 CHARGER

*PRODUCT TYPE: PORTABLE WIRELESS POWER
TRANSFER DEVICE*

Report Number: 90976808 Appendix D

Date: 24 JAN 2023

Prepared by:

Luke Snow, Senior Design/Product Development Engineer

Jeremiah Darden, Senior Development Quality Engineer

Summary of Evaluation.....	3
Objective	3
Computational Summary Results.....	6
SAR RF Exposure Evaluation.....	7
Overview	7
Compliance with FCC 2.1093	7
Limits.....	7
Assessment	8
Measurement Uncertainty.....	17
Code Verification and Validation	34
Evaluation Process and Results.....	36
END OF DOCUMENT.....	44

Definitions

RSS	Root Sum Square
W	Watts
A/m	Amps per meter
dB	decibel
dBm	decibel-milliwatts
cm	centimeters
Mm	millimeters
In	inches
kHz	kilohertz
Hz	Hertz
RMS	Root Mean Squared
V/m	Volts per meter
W/kg	Watts per kilogram
WPT	Wireless Power Transfer
IPG	Implantable Pulse Generator
FEM	Finite Element Method



Abbott Laboratories

Neuromodulation

6901 Preston Rd.

Plano, TX 75024

800-727-7846

Summary of Evaluation

Standards

Specification	Method	Notes
FCC 2.1093:2022	FCC Inquiry SPR-002 Issue 2	Per 2.1093 Radiofrequency radiation exposure evaluation: portable devices. (d)The SAR limits specified in § 1.1310(a) through (c) of this chapter shall be used for evaluation of portable devices transmitting in the frequency range from 100 kHz to 6 GHz.

Overall Results

Method Clause	Description	Applied	Result	Comments
1.1307 (b) (1) (i) (B)	SAR Evaluation for human RF exposure pursuant to § 1.1310 using Computational Analysis. KDB 865664 D02 RF Exposure Reporting v01r02	Yes	Pass	Method from FCC Inquiry for ICES SPR-002 Numerical Computational SAR for Head/Torso. FCC 1.1310 (c) limit applied.

Executive Summary

Computational analysis using finite element method was used to simulate the specific absorption rate over one gram of tissue with passing results. The computational process from the listed methods includes identifying the exposure conditions of the device under test, building the model within the code validated simulation software and then validating the model with actual measurements using an H-field loop probe. Once the measurement uncertainty was established, the computational simulation was performed, and the results were compared to the limits specified within this document. All applicable results passed.

Objective

Show SAR compliance for Wireless Power Transfer device operating below 4MHz.

EUT Use-Cases and key RF exposure conditions

SUMMARY: The following RF Exposure conditions are used for the assessment documented in this report	
Intended Use	Portable
Location on Body	Torso
How is the Device Used	< 20cm, on the body
Radio Under Evaluation	WPT (266kHz-320kHz)
Body Worn Accessories	The charging apparel (model 16750 or 16760) are intended to secure the Gemini Charger (model 16000) at the pulse generator implant location. The accessories are made of spandex and fabric and do not include any RF shielding.
Environment	General Population/Uncontrolled Exposure

Product Description and Intended Use

The portable charger is a wireless power transfer device (WPT) that employs charging frequencies between 266 kHz and 320 kHz. When initially powered on, the charger sweeps across the frequencies from 320 kHz down to 266 kHz, with the peak output power achieved at approximately 280 kHz. The frequency continues sweeping until the charger is aligned over the IPG and begins actively charging. Once actively charging, the frequency is fixed at a constant narrowband wavelength. If an IPG is not aligned within a couple minutes, the charger will shut off and any WPT signals are discontinued. Typical IPG charging time ranges from 30min to typical overnight period of 7 hours.

Rated power delivered to inductive coil:	1.3 Watts
Power accuracy:	+/- 0.5 dB
Frequency of operation:	266 kHz – 320 kHz
Duty cycle:	100% duty cycle
Largest Product Dimension:	3.9 inches

Charger Intended Use

Charger: The charging system is intended to be used to charge the Gemini rechargeable implantable pulse generator (IPG), also referred to as a generator.

The charging apparel (model 16750 or 16760) are intended to secure the Gemini Charger (model 16000) at the pulse generator implant location.



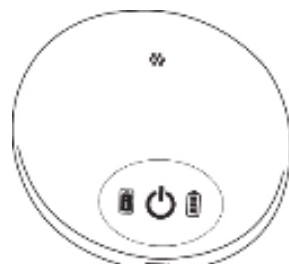


Figure A Charger Diagram (Model 16000)

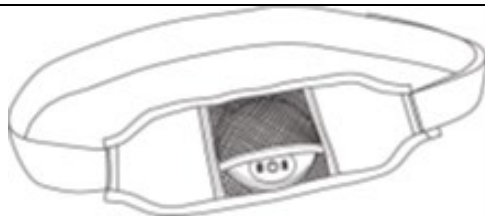


Figure B Charger Apparel Abdominal Diagram 1

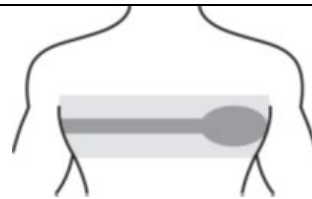


Figure C Abdominal Usage Example

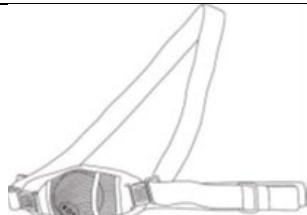


Figure D Charger Apparel Thoracic Diagram 2

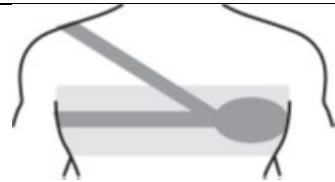


Figure E Thoracic Usage Example



Figure F Charger Apparel Thoracic Diagram 3

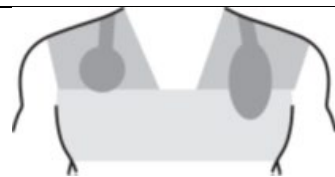


Figure G Thoracic Usage Example



Abbott Laboratories

Neuromodulation

6901 Preston Rd.

Plano, TX 75024

800-727-7846

Computational Summary Results

Limit Type	FCC 1.1310 (c) United States of America Limit	RSS-102 Table 2 & 3 /SPR-002 Canada Limit	62311/(1999/519/EC) (EU)/International Limit	Results	Pass/Fail
SAR (W/kg)	1.6	1.6	2.0	0.11 W/kg	Pass
Internal Instantaneous E-Field (V/m RMS)	N/A for 1.1310(c)	35.9	N/A for Basic restrictions	16.1 V/m	Pass
<p>Note 1: E-Field limit calculated with lowest device operating frequency of 266kHz. f= frequency in Hertz. $1.35 \times 10^{-4} \times f$</p> <p>Note 2: 100% duty cycle results are reported. SAR Averaging time is not applicable for the purposes of this FEM computational SAR. See the Assessment section of this report for more detail.</p>					



Abbott Laboratories

Neuromodulation

6901 Preston Rd.

Plano, TX 75024

800-727-7846

SAR RF Exposure Evaluation

Overview

SAR results that are under the 47 CFR 1.1310 (c) limits for human RF exposure for localized SAR are considered to be compliant to FCC 2.1093 for portable devices used against the head/torso. As stated, “(d) The SAR limits specified in § 1.1310(a) through (c) of this chapter shall be used for evaluation of portable devices transmitting in the frequency range from 100 kHz to 6 GHz.”

Compliance with FCC 2.1093

§ 2.1093 Radiofrequency radiation exposure evaluation: portable devices.

(b) For purposes of this section, the definitions in § 1.1307(b)(2) of this chapter shall apply. A portable device is defined as a transmitting device designed to be used in other than fixed locations and to generally be used in such a way that the RF source's radiating structure(s) is/are within 20 centimeters of the body of the user.

(d)

(1) Applications for equipment authorization of portable RF sources subject to routine environmental evaluation must contain a statement confirming compliance with the limits specified in § 1.1310 of this chapter as part of their application. Technical information showing the basis for this statement must be submitted to the Commission upon request. The SAR limits specified in § 1.1310(a) through (c) of this chapter shall be used for evaluation of portable devices transmitting in the frequency range from 100 kHz to 6 GHz. Portable devices that transmit at frequencies above 6 GHz shall be evaluated in terms of the MPE limits specified in Table 1 to § 1.1310(e)(1) of this chapter. A minimum separation distance applicable to the operating configurations and exposure conditions of the device shall be used for the evaluation. In general, maximum time-averaged power levels must be used for evaluation. All unlicensed personal communications service (PCS) devices and unlicensed NII devices shall be subject to the limits for general population/uncontrolled exposure.

(2) Evaluation of compliance with the SAR limits can be demonstrated by either laboratory measurement techniques or by computational modeling. The latter must be supported by adequate documentation showing that the numerical method as implemented in the computational software has been fully validated; in addition, the equipment under test and exposure conditions must be modeled according to protocols established by FCC-accepted numerical computation standards or available FCC procedures for the specific computational method. Guidance regarding SAR measurement techniques can be found in the Office of Engineering and Technology (OET) Laboratory Division Knowledge Database (KDB). The staff guidance provided in the KDB does not necessarily represent the only acceptable methods for measuring RF exposure or RF emissions, and is not binding on the Commission or any interested party.

The device under test evaluation will be used with a separation distance of less than 20 centimeters between the antenna coil and the body of the user or nearby persons and must therefore be considered a portable transmitter power 47 CFR 2.1093(b). Per 2.1093(d), limits from 1.1310 are used and computational analysis can show compliance.

Limits

§ 1.1310 Radiofrequency radiation exposure limits.

(a) Specific absorption rate (SAR) shall be used to evaluate the environmental impact of human exposure to radiofrequency (RF) radiation as specified in § 1.1307(b) of this part within the frequency range of 100 kHz to 6 GHz (inclusive).



Abbott Laboratories

Neuromodulation

6901 Preston Rd.

Plano, TX 75024

800-727-7846

(c) The SAR limits for general population/uncontrolled exposure are 0.08 W/kg, as averaged over the whole body, and a peak spatial-average SAR of 1.6 W/kg, averaged over any 1 gram of tissue (defined as a tissue volume in the shape of a cube).

Exceptions are the parts of the human body treated as extremities, such as hands, wrists, feet, ankles, and pinnae, where the peak spatial-average SAR limit is 4 W/kg, averaged over any 10 grams of tissue (defined as a tissue volume in the shape of a cube). Exposure may be averaged over a time period not to exceed 30 minutes to determine compliance with general population/uncontrolled SAR limits.

(d)

(1) Evaluation with respect to the SAR limits in this section must demonstrate compliance with both the whole-body and peak spatial-average limits using technically supported measurement or computational methods and exposure conditions in advance of authorization (licensing or equipment certification) and in a manner that facilitates independent assessment and, if appropriate, enforcement. Numerical computation of SAR must be supported by adequate documentation showing that the numerical method as implemented in the computational software has been fully validated; in addition, the equipment under test and exposure conditions must be modeled according to protocols established by FCC-accepted numerical computation standards or available FCC procedures for the specific computational method.

For 100kHz to 6GHz and a test separation distance of 0.5 centimeters, the limit for head and body SAR is for 1 gram of tissue for portable devices.

Assessment

Overview: Computational Analysis follows ISED SPR-002 using Finite Element Method (IEC/IEEE 62704-4)
Model and Analysis: The computational model and analysis was performed using Ansys HFSS that has gone through code verification and validation per SPR-002 and applicable clauses of 62704-4 for Finite Element Method analysis.
Software Version: ANSYS Electronics Desktop 2022 R2.
Computational Resources: Simulations were performed on a computer with 32 cores CPU and 488 GB RAM. The minimum requirement to reproduce the results is 37.8 GB RAM for adaptive meshing and frequency analysis. The mesh is length-based setting with the surface deviation of gap/2, in which the gap is the distance between closest coil turns. This will account for a reasonable mesh on the coil so that it will not “merge” the coil in the smallest distance. The boundary is an absorbing radiation boundary box with size of 2 m x 2 m x 2 m. The center of the box is the same as the coil center. The total simulation time was approximately 113 minutes. The general setup is 8 passes max at frequency 280 kHz. The max magnitude of delta S is 0.02. The mesh is set to adaptive with max 30% of the refinement per pass. The minimum number of converged passes is 1 and the number of passes is 8. The coil inductance was also added in the expression cache. The simulation completed on the 8th pass and the max magnitude of delta S is 8.3 e-05 (< target 0.2). The total number of mesh element is 963418.

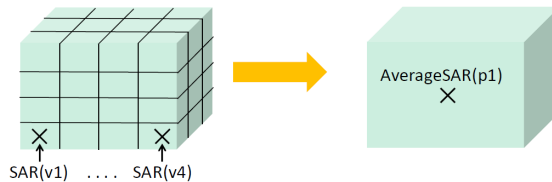
List of key computational parameters:

Parameter	Value
Ansys HFSS Avg SAR method	IEC/IEEE 62704-4
Cell size	1cm
Voxel size	1mm
Domain size	2m x 2m x 2m
Boundary	Radiation boundary
Phantom distance to boundary (min/max)	90cm / 140cm
Time step size	N/A*
Tissue / device separation	3.2mm
Material density	1 gram / cm ³
Mass of tissue	1 gram

*FEM method of solution is in frequency domain and is therefore steady state.

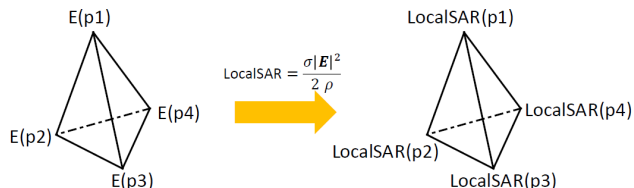
Average SAR 62704-4

- The density and localSAR values are mapped over the grid of voxels
- The average SAR for each voxel is calculated: SAR(v1), SAR(v2)...
- The average SAR in the averaging volume is then found using the SAR values of each voxel


Ansys
©2020 ANSYS, Inc. / Confidential

Local SAR

- LocalSAR is calculated at each mesh point



- LocalSAR is not averaged over a volume
- HFSS computes localSAR at each mesh point on an overlay plot. Values between the mesh points across the plot are interpolated.

Ansys
©2020 ANSYS, Inc. / Confidential



Abbott Laboratories

Neuromodulation

6901 Preston Rd.

Plano, TX 75024

800-727-7846

Phantom and Material Properties:

The body phantom reference parameters specified in IEC/IEEE 62209-1528 and ASTM F2182-09 were used, as directed by SPR-002. The tissue and dielectric parameters are also specified in SPR-002. As per IEC/IEEE 62704-4, since the phantom used in the model is a reference phantom, the phantom uncertainty is zero.

To represent intended use, the charger will be placed on a body torso (back or front chest). The torso was modelled as a flat elliptical phantom with cross-sectional parameters as defined in IEC/IEEE 62209-1528, and the height parameter specified as defined in ASTM F2182-09. The phantom flat bottom had the shape of an ellipse with a length of 600 mm and a width of 400 mm, and the height was 650mm. Since this was a simulation model, the thickness of the container wall in the phantom could be neglected and was set to be zero. The volume of the phantom was enough to calculate SAR over 1 g or 10 g of the tissue. According to IEC/IEEE 62209-1528, the dielectric constant was 55. The electrical conductivity was 0.75 S/m. And the mass density was 1000 kg/m³. Although the requirements in standards are limited to ≥ 4 MHz, the material properties above may be used below 4 MHz for the purpose of SPR-002.

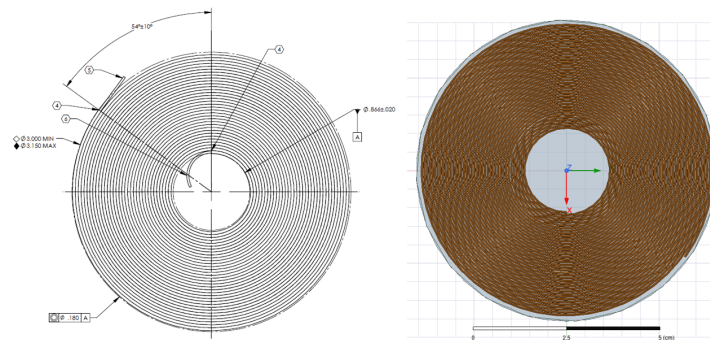
Coil and Model Characteristics:

The EUT model is a Charger coil with a tuning capacitor. From the manufacturing specification, the Charger coil is a spiral copper wire with 40 turns. Each wire is made of 250 strands of 46 AWG bonded Litz wire. The outer diameter of the coil is 3 inches to 3.150 inches. The inner diameter is 0.866 ± 0.20 inches. The maximum thickness of the coil is 0.039 inches. The inductance of the coil, with ferrite backing included, is $120 \mu\text{H} \pm 5\mu\text{H}$ at 300 kHz and the AC resistance of the Litz wire coil windings is 1.5 ohms. To model the Charger coil in HFSS, a spiral geometry was drawn natively in the HFSS CAD interface to facilitate the cleanest possible mesh. The native spiral object in HFSS was used, with an inner radius of 11.3 mm, a turn spacing of 0.71 mm, and $N = 39.85$ turns (the fractional turn number is used to precisely place the termination points on the inside and outside of the coil relative to each other). Also, for simplicity, the coil was modeled as a single solid copper wire with a circular cross section of radius 0.3 mm instead of attempting to model the litz wire in detail. The gaps between wires in the single wire model will only affect field readings extremely close to the coil (on the order of 0.5mm), and therefore will not affect the SAR results. To further facilitate meshing, the circular cross section of this single wire was segmented into six segments, rather than using a pure curvilinear cross section. The copper of the coil wire was modeled using the default HFSS approach of a surface mesh with finite conductivity boundary and no interior fields ("solve on surface" for conductors). All these modeling choices facilitate reasonable simulation complexity while still achieving the desired coil inductance at the frequencies in question. The inductance is considered the most important aspect of the coil performance to replicate before using the coil model in subsequent SAR calculations. The simulation shows that the coil inductance is 117 μH at 300 kHz with a resistance of 1.4 ohms, which is aligned with the manufacturing specification (120 $\mu\text{H} \pm 5\mu\text{H}$ at 300 kHz, 1.5 ohms). Therefore, the simulated coil model is valid. The product requires that the charger coil assembly shall have a resonant frequency of $277.1 \text{ kHz} \pm 2.5 \text{ kHz}$. Therefore, a capacitor was added in series with the coil in the Ansys Circuit to achieve the resonance. The capacitor value is 4.2985 nF and the resonant frequency is 276.81 kHz.

Modeled and test device near-field radiating characteristics should be similar, since the geometries match closely, and the simulated inductance falls within the measured inductance min/max values. This is confirmed via measurement and predicted field-strength overlays, as shown in the report.

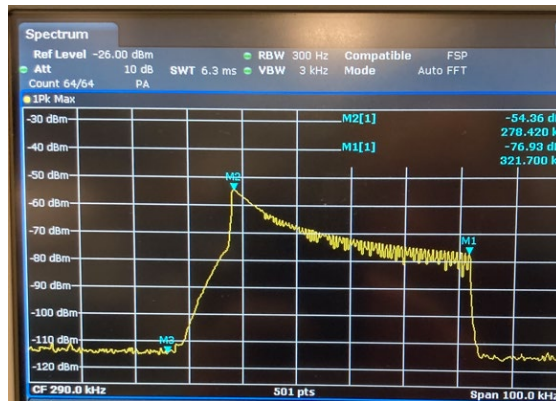
The tested and modeled device parameters are tabulated below. Refer to the figure below.

Property	Test device	Model
Coil outer radius	3.11 in	3.12 in
Coil inner radius	11 mm	11.3 mm
Wire radius/Litz wire	1 mm	0.7 mm
Inter-winding gap	Negligible	0.3 mm
Turns	40	39.85
Coil winding start/finish angle	54 deg	54 deg
Ferrite permeability	120	120
Ferrite diameter	3.2 in	3.2 in
Ferrite thickness	0.052 in	0.051 in
Coil inductance w/ ferrite backing	120 μH	117 μH
Coil AC resistance	1.5 ohms	1.4 ohms

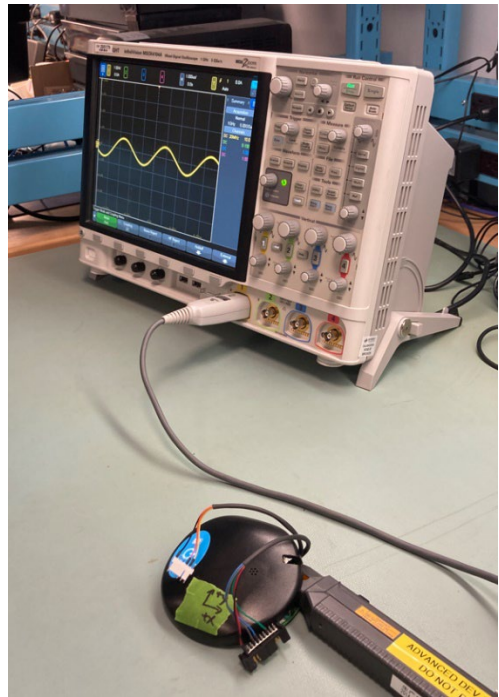


Excitation:

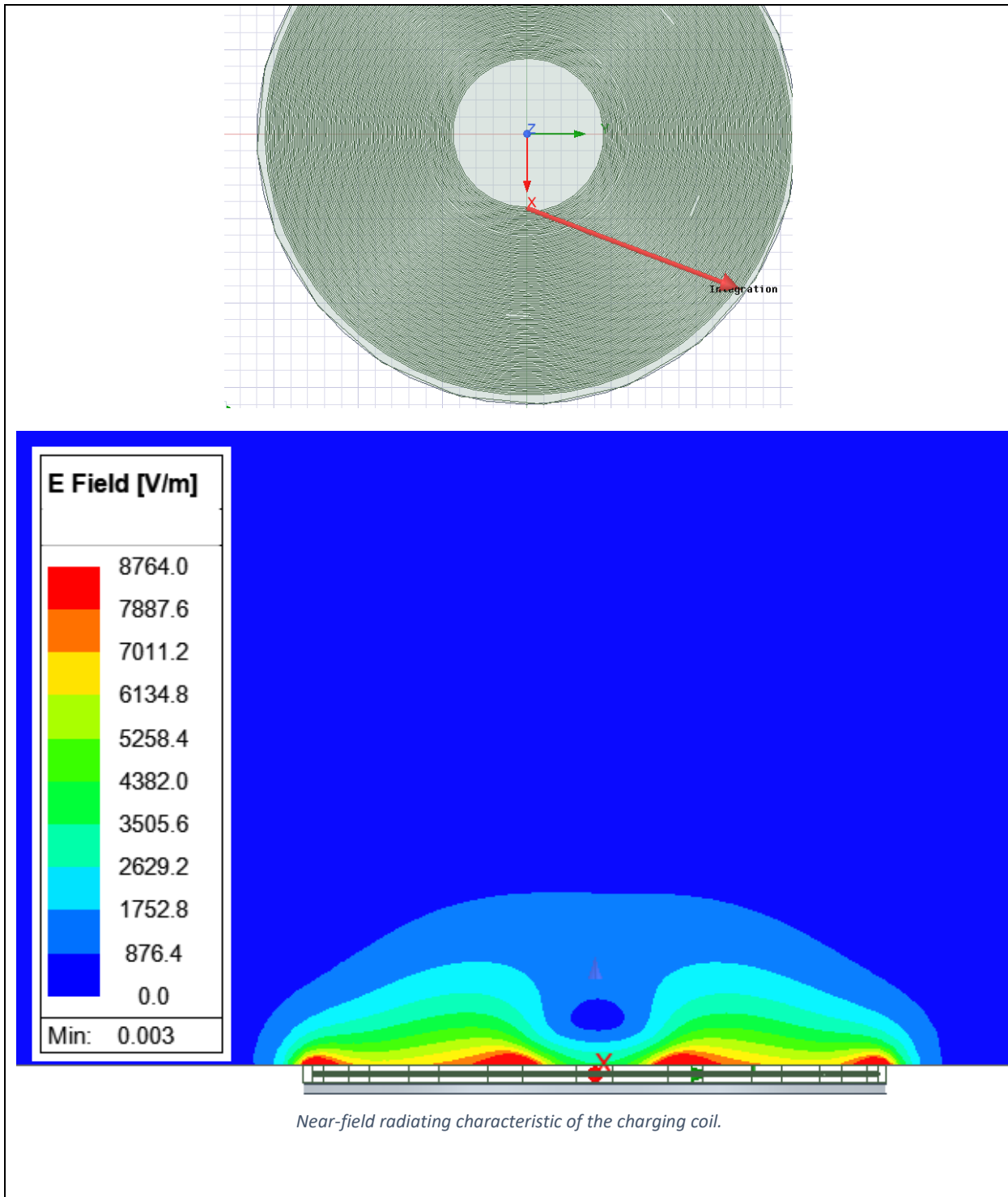
The excitation current used in the model was based on bench measurements in the lab. The frequency at which the maximum field occurs is approximately 280kHz, which was determined by using a loop probe connected to a spectrum analyzer in the “max-hold” setting. The output of this measurement is shown below.



The setup for measuring the excitation current used for the model validation field measurements included an oscilloscope, a clamping current probe, and DUT 143711001498 with a PCB to Coil jumper wire that allows current probe measurements. The DUT was put into a CW charging mode and an input current of 1.7A peak-to-peak was measured, as shown. The oscilloscope (EM. No. 205179) used for the measurement was in-cal up through Feb. 2023.



This measurement was used to set the AC magnitude in the Ansys HFSS model simulation. The ground in the coil was at the ending point on the inner coil diameter, and the higher potential side was on the edge of the coil.



Rationale for SAR on Non-Body Side

The primary use-case is when the charging coil is facing into the body. An additional scenario is the case where the charger is placed so that the coil is facing outwards, away from the body. A consideration of the E-field on both sides of an unloaded coil will be used to show that SAR is negligible if the coil is pointed away from the body.

In addition to the ferrite, there is a ground plane above the ferrite due to the PCB inside the plastic enclosure. In the real DUT, this ground plane will dramatically block the E-field from the non-body side.

In-lieu of checking the SAR directly, the magnitude of the E-field is calculated and compared for the body and non-body side using the validation model. Refer to diagrams below. The E-field on the body side of the phantom tissue has a peak E-field of around 7600 V/m. On the non-body side of the phantom, the E-field levels are less than around 3000-4000 V/m. Refer to diagrams below.

The lower E field strength on the non-body side of the coil compared to the body side of the coil, and the fact that there is a ground plane PCB placed close to the coil in the real DUT, leads us to conclude that the SAR on the non-body side is less than the body side.

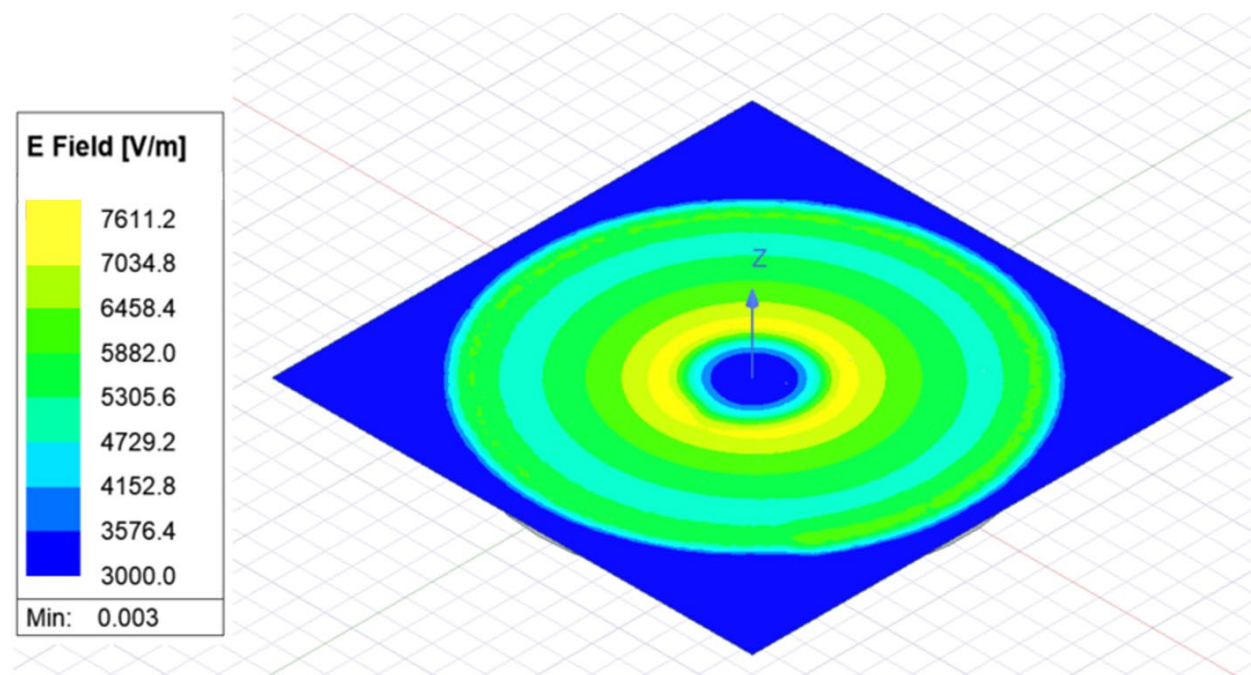


Figure H Body-side of coil, validation model.

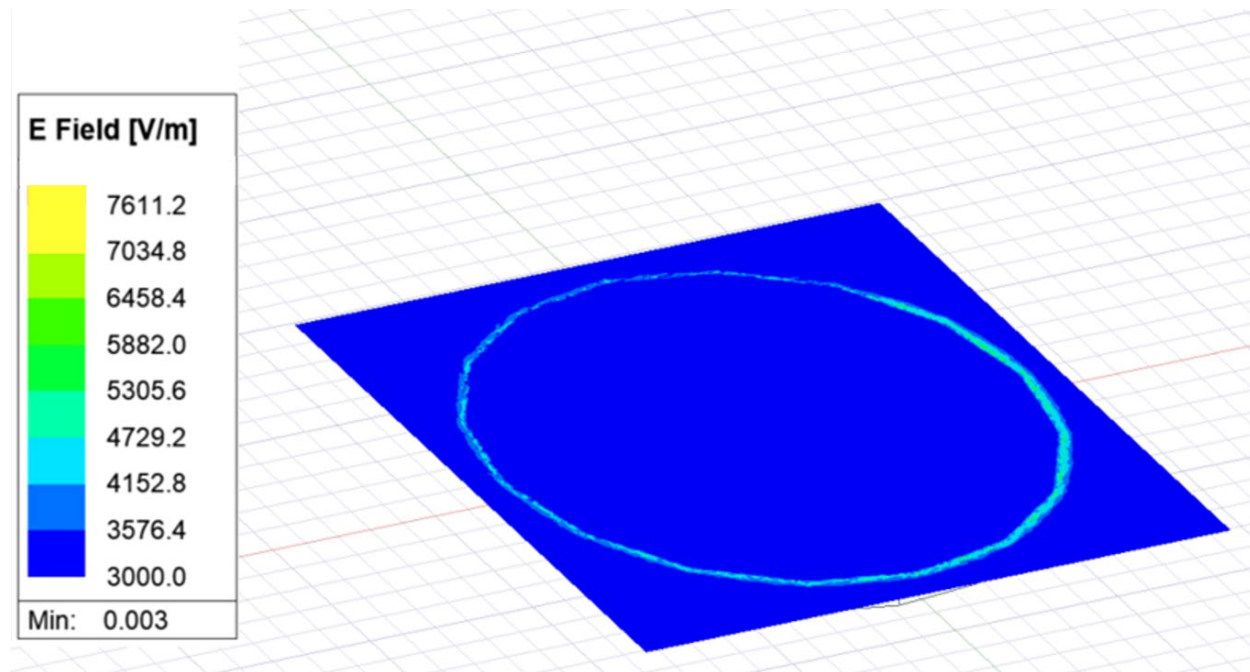


Figure I Non-body side of coil, validation model, bottom perspective.

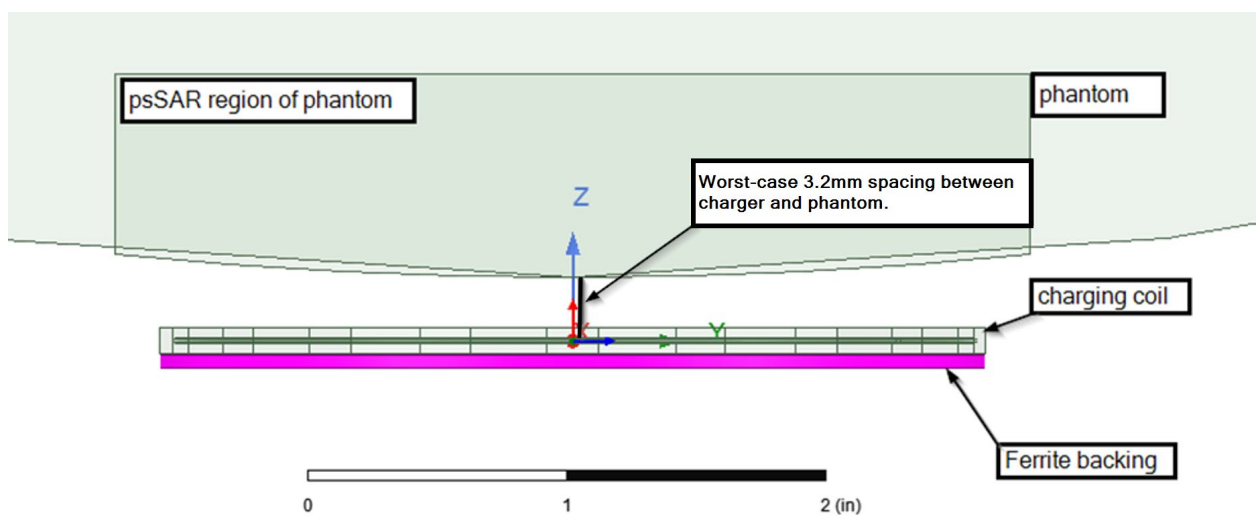


Figure J Worst-case DUT position is at 3.2mm from the surface of the phantom.

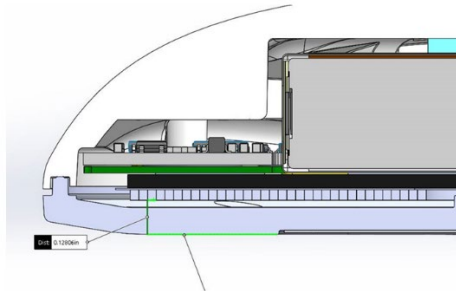


Figure K Enclosure and Air Gap distance from Coil

Assessment Against Basic Restrictions (Section 8.4.1 of SPR-002, issue 2)

SAR

The SAR-based exposure ratio is calculated as per SPR-002 issue 2, using the following equation:

$$ER_{SAR-BR} = \frac{1}{SAR_{BR}} \sum_{n=1}^N SAR(f_n)$$

- $SAR_{BR}=1.6$ W/kg, since the implant is installed in the lower back or upper torso.
- $N=1$, since the worst case occurs at a single frequency (~280 kHz).
- Duty cycle is 100%.

Time Averaging

The SAR simulation is solved in the frequency domain, and therefore the result is steady state in the time domain. The DUT output was set to a constant frequency and output level. The frequency and power level were the worst-case that the DUT can produce. Therefore, the 30-minute time averaged SAR is no different from the 6-minute averaged SAR.

Internal E-field

The NS-based or SAR-Based E-Field exposure ratio can be calculated as follows:

$$ER_{NS-BR} = \sum_{m=1}^M \frac{E_{int}(f_m)}{E_{BR}(f_m)}$$

The calculation is performed the same as SAR, and with the same worst-case assumption that frequency is 280 kHz, and duty cycle is 100%.

Measurement Uncertainty

Uncertainty Summary (SPR-002 Issue 2, section 8.3.5)

Uncertainty Component	Subclause	Uncertainty (%)
Uncertainty of the DUT model with respect to simulation parameters	7.2	0.4%
Uncertainty of the developed numerical model of the DUT	7.3	13.0%
Combined std. uncertainty (k=1)		13%
Expanded std. uncertainty (k=2)		26%
Expanded Uncertainty is less than 30% per SPR-002 and IEC 62311		

Figure L Expanded uncertainty

Uncertainty Method

Uncertainty of numerical model algorithm (Related: Section 7.2.1 of IEC/IEEE 62704-4:2020)

The uncertainty for each of the following quantifies in this section are combined into an aggregate uncertainty.

Mesh convergence (Related: Section 7.2.2 of IEC/IEEE 62704-4:2020)

Since the model is constrained only to solve first order elements, simulation setups are run until the following criteria is met:

- Adaptive passes were performed until the number of mesh elements has increased by at least 50%
- The denser mesh M' edge minimum/maximum lengths in the psSAR region are less than half the corresponding edge lengths of the less dense mesh, M (Note: this condition was not met for the antenna region, due to the tight meshing of the coil, present from the earlier adaptive passes)
- The location of the electric field maximum in the psSAR region of mesh M' does not deviate by more than the minimum edge length of the electric field maximum within the psSAR region of mesh M
- The maximum psSAR deviation is given as an uncertainty with rectangular probability distribution

Open Boundary Conditions (Related: Section 7.2.3 of IEC/IEEE 62704-4:2020)

The size of the simulation domain was increased by 50% (as allowed, per section 8.3.5.2 in SPR-002 issue 2). The maximum deviation of the psSAR is recorded.

Power Budget (Related: Section 7.2.4 of IEC/IEEE 62704-4:2020)

The power accepted into the system is compared against the dielectric, conductive, and radiated losses in the system. The deviation input/output power is reported as the same percent deviation in SAR.

Convergence of psSAR sampling (Related: Section 7.2.5 of IEC/IEEE 62704-4:2020)

The relative difference of the psSAR between the last, and step preceding the last adaptive pass is reported as an uncertainty with rectangular probability distribution.

Dielectric Parameters of the Phantom (Related: Section 7.2.6 of IEC/IEEE 62704-4:2020)

As per SPR-002 issue 2 section 8.3.5.2, this uncertainty is set to 0 percent, since the flat cylindrical phantom of IEC/IEEE 62209-1528:2021 is used.

Uncertainty of the DUT model (Related: Section 7.3.3 of IEC/IEEE 62704-4:2020)

Calculate the DUT uncertainty as per equation below

$$U_{|E|^2,d} [\%] = 100 \cdot \max \frac{\left| |H_{ref}(n)|^2 - |H_{num}(n)|^2 \right|}{|H_{ref,max}|^2}$$

The default location of the device under test, d_0 , was taken to be 3.2mm along the Z-axis, above the probe. Due to the practical considerations, such as the probe size and proximity of the DUT, the measurement distances shown below were taken, rather than those specified in the related section of IEC/IEEE 62704-4:2020 (e.g., 0.5 d_0 , 1.5 d_0 , etc.).

Measurement along Z-axis	Numerical predicted loop probe output power along Z-axis (dBm)
0.26"	-29.6
1.40"	-45.1
1.64"	-48.0

Figure M DUT uncertainty calculation inputs.

The predicted values, as well as the measurements, are tabulated according to the above equation to obtain an uncertainty. The worst-case uncertainty of these calculations is taken. This uncertainty is combined, via root-sum-square, to obtain an overall uncertainty budget for the DUT model.

Uncertainty of the Phantom model (Related: Section 7.3.4 of IEC/IEEE 62704-4:2020)

The flat cylindrical phantom of IEC/IEEE 62209-1528-2021 is used, and therefore the uncertainty of this term is 0%.

Uncertainty of the measurement equipment and procedure (Related: Section 7.3.3 of IEC/IEEE 62704-4:2020)

The uncertainty of the loop probe and procedure was determined by taking multiple measurements at the same location between setups, i.e., measurements at a given position were not consecutive. For example, a z-axis measurement at position 0 was performed, other measurements were performed that involved moving the probe, and then when performing the planar measurements, position 0 the output power was measured again. The probe specified within SPR-002 Section 7.1 has specifications not readily available on the market at the time of SPR-002 Issue 2 release, so an alternative probe was used over the positions specified. The Beehive 100A has a Tip Diameter of 0.5 inches (~1.3cm), a Loop Diameter of 0.4 inches (~1.0cm) and a probe tip thickness of 0.11 inches (~0.3cm). The loop probe has an integrated electrostatic shield, providing isolation from common mode signals. The additional uncertainty of this probe was factored into the validation. Validation measurements are from Element Report "ABBO0234" (Element A2LA ISO 17025 Cert # 3310.03) which include applicable equipment calibration and measurement details.

BeeHive 100A probe, z-axis measurements	
position	position (inches)
pos0	1.64
pos1	2.64
pos2	3.64

Figure N Uncertainty of the equipment and measurement procedure.

Model validation (Related: Section 7.3.5 of IEC/IEEE 62704-4:2020, Section 8.3.2 of SPR-002, Issue 2)

The model is considered valid if the following equation is true for all points measured:

$$E_n = \sqrt{\frac{(v_{sim,n} - v_{ref,n})^2}{(v_{sim,n} U_{sim(k=2)})^2 + (v_{meas,n} U_{meas(k=2)})^2}} \leq 1$$

All points within 5% of the peak value, or 13 dB, measured are required to be evaluated using this equation. Additional points, however, that were more than 13 dB below peak were taken to include enough points to validate the model down to the observed noise-floor. Overlay plots between the predicted and measured loop probe output power due to the H_z-fields are also provided.

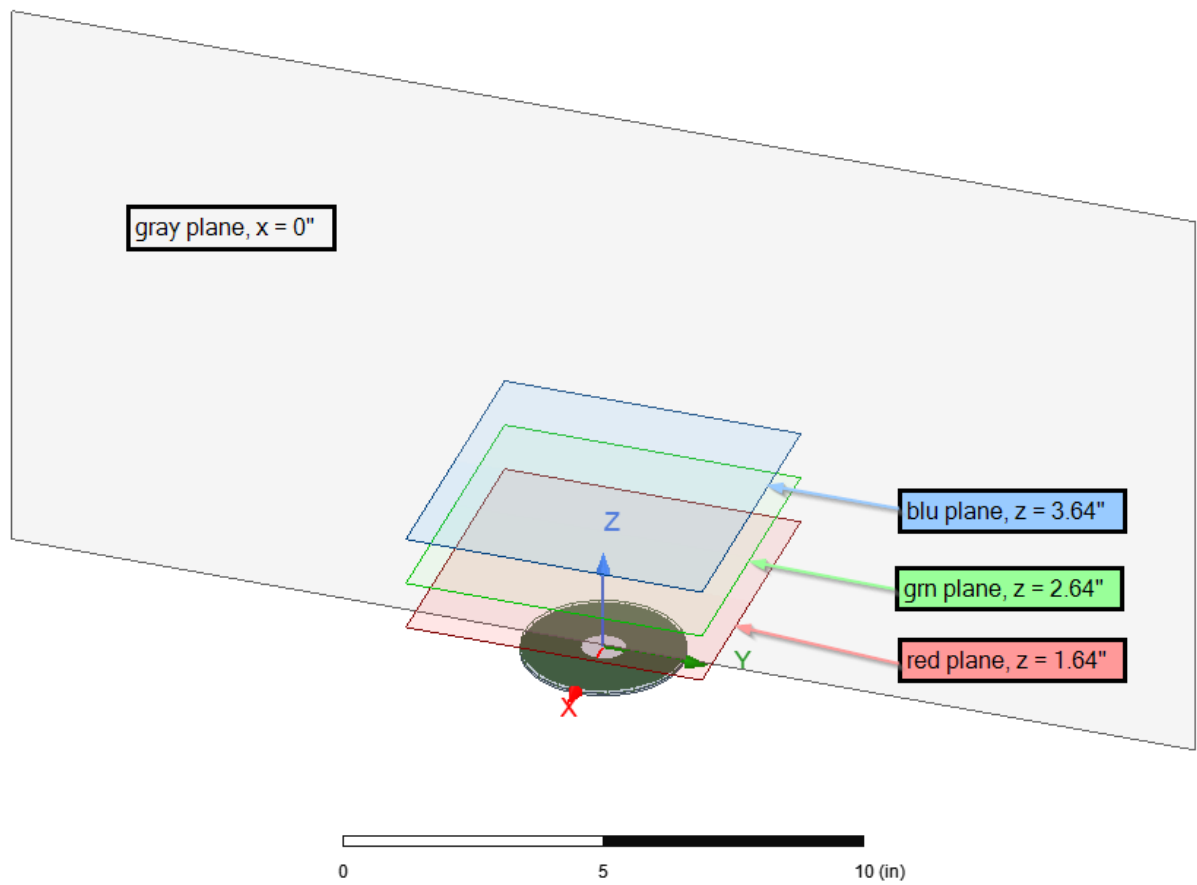


Figure O Measurement planes: Measurements taken along z-axis, as well as the x-axis at a constant z-value

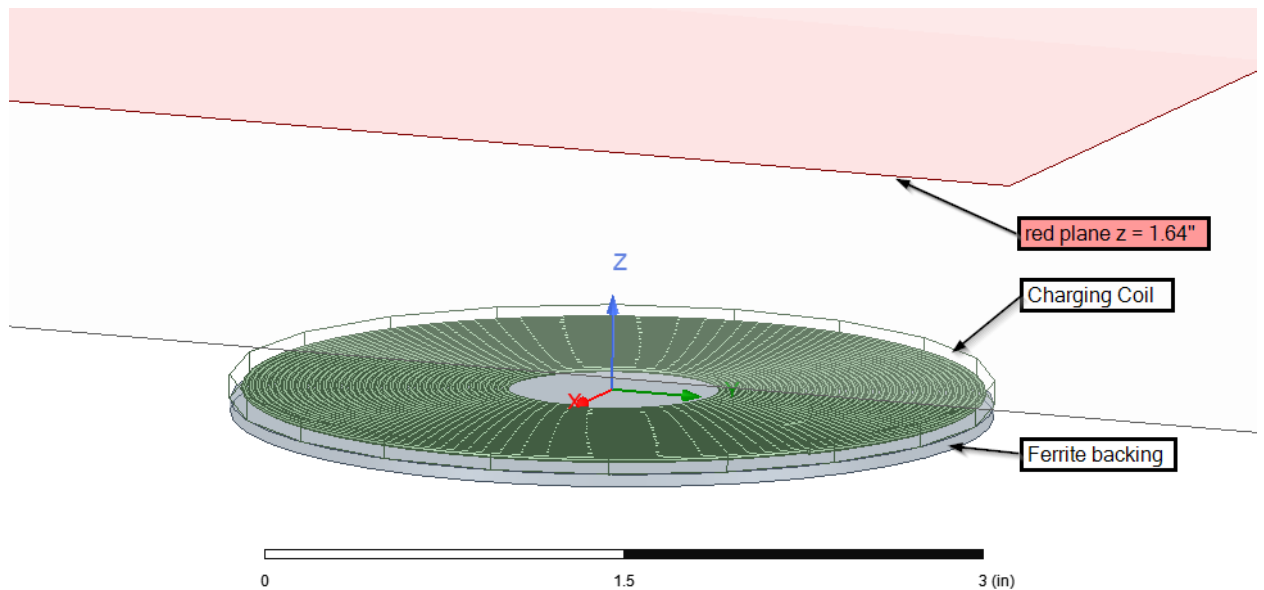


Figure P Close up of DUT with red ($z=1.64"$) measurement plane

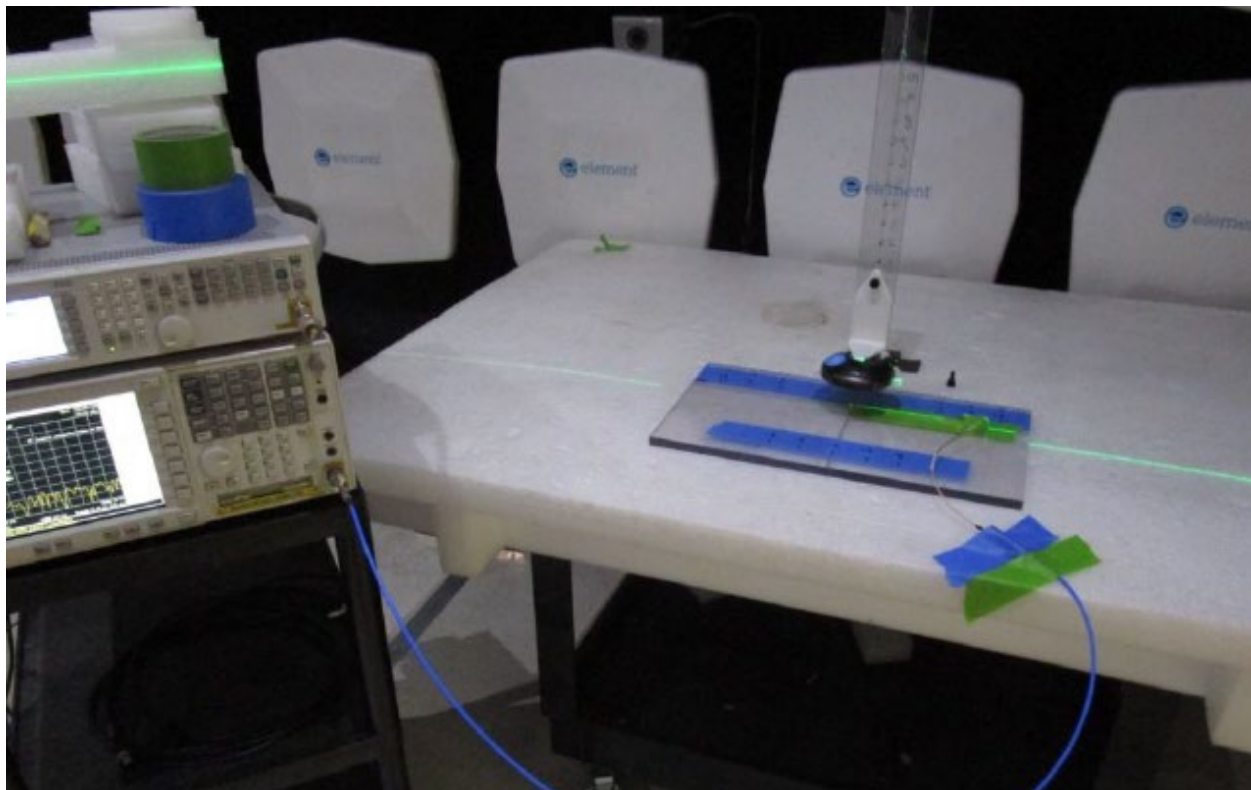


Figure Q - Validation measurement setup

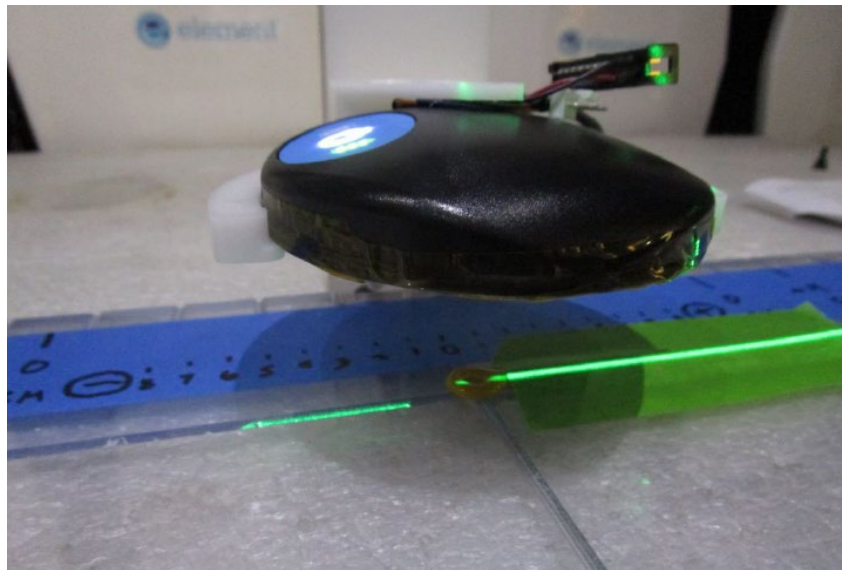


Figure R - DUT and Beehive 100A Measurement Probe

Overall assessment of uncertainty (Related: Section 7.4 of IEC/IEEE 62704-4:2020)

The uncertainty of numerical model algorithm and the uncertainty of the DUT model are combined, via root-sum-square calculation, to generate a combined ($k = 1$) and expanded ($k = 2$) uncertainty. The expanded uncertainty must be less than 30%.

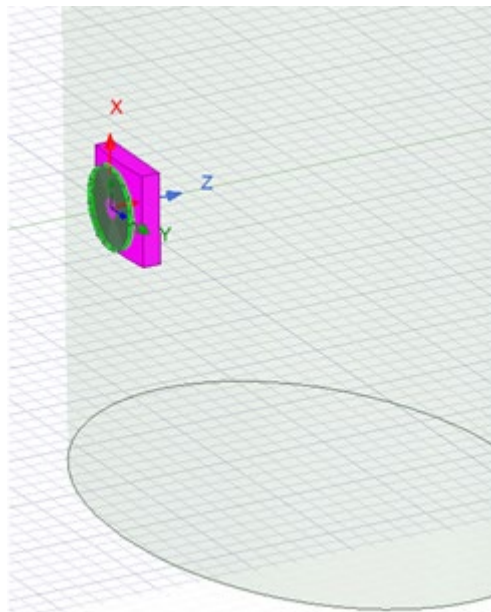


Figure S Numerical model used to check mesh convergence, psSAR region shown.



Abbott Laboratories

Neuromodulation

6901 Preston Rd.

Plano, TX 75024

800-727-7846

Uncertainty Analysis

Mesh convergence

Setup	No. Elements
1	296927
8	963418
tolerance	67%

Figure T Number of mesh elements and percent increase of elements between setup1 and setup8.

SAR region		
Setup	min edge	max edge
1	6.6	45
8	0.6	12.7
qty M' / qty M	10%	28%

Figure U Comparison of denser mesh M' (setup 8) and less dense mesh M (setup 1).

	Location			Peak E-field max
M' (E-field max)	0.004	0.021	0.013	22.8
M (E-field max)	0.004	0.004	-0.024	18.4
Deviation of E-field max location =====>				
min mesh edge length in psSAR region of M. =>				
Deviation of E-field max location < minimum mesh edge length.?				
Yes (Valid)				

Figure V Change of location of Peak E-field max over adaptive passes

SAR deviation, Uniform distribution

Setup	Max Local SAR (W/kg)
a_- (adaptive pass 8) max SAR	0.196
a_+ (adaptive pass 1) max SAR	0.208
mu	0.006
Uncertainty	0.4%

Figure W Deviation of maximum local SAR between setup 1 and setup 8.

Open Boundary Conditions, Maximum deviation of target quantity

model	setup	sweep	edge length (m)	psSAR (W/kg)
baseline	8	1	1.0	0.19564
expanded boundary	8	1	1.5	0.19562
uncertainty			0.01%	

Figure X Uncertainty due to expansion of simulation domain by 50%.

Power Budget

conductor losses	1.40	Watts
dielectric losses	0.01	Watts
radiated power	3.09E-06	Watts
conductor loss + dielectric loss + radiated	1.413	Watts
accepted power	1.417	Watts

Table 1 – Power budget

uniform distribution over all adaptive pass

a_- (baseline)	1.413
a_+ (expanded)	1.417
mu	1.42
a	0.002
uncertainty	0.1%

Figure Y Uncertainty due to discrepancy between losses and radiated power and accepted power.

Convergence of psSAR sampling

Setup	Maximum SAR
7	0.1954
8	0.1956
tolerance	0.1%

Figure Z Uncertainty due to change in max SAR

Simulation uncertainty

Uncertainty component	Subclause	Uncertainty (%)
Mesh convergence	7.2.2	0.4%
Open boundary conditions	7.2.3	0%
Power budget	7.2.4	0.1%
Convergence of psSAR sampling	7.2.5	0.0%
Phantom dielectrics*	7.2.6	0.0
Combined std. uncertainty (k=1)		0.4%

*Uncertainty = 0%, as Elliptical flat reference phantom of IEC/IEEE 62209-1528 is used.

Figure AA Aggregate simulation uncertainty.
Uncertainty of the measurement equipment and procedure

(Related: Section 7.3 of IEC/IEEE 62704-4:2020 According to Manufacturer Specification)

Equipment Validation:

For the measurement equipment, validation has multiple steps. Due to the size of the DUT, a H-Field probe capable of small spatial resolutions relative to the DUT's 9.9cm diameter was used (Beehive Model 100A with a loop coil diameter of 1cm). To check its accuracy, measurements were first taken within a Helmholtz coil. The Helmholtz coil field strength and uniformity were checked with a calibrated H-Field probe (Wavecontrol SMP-2 meter with Model WP400 probe). The 3-axis isotropic probe had a loop diameter of 12.8cm. The uniformity volume was approximately 8000 cm³ (20cm x 20cm x 20cm) so the isotropic probe fits within the volume when placed at the center. 27 evenly spaced positions around the volume were measured. The positions with the highest and lowest field values varied +/- 0.2 A/m from the field value at the center position. Once the uniformity was established, the calibrated probe was again placed at the center of the uniform volume. This measurement was recorded. The calibrated probe was removed and replaced with the 1cm probe connected to a measurement receiver via a shielded coaxial cable. The measurement was recorded. The two values were compared and factored into the measurement equipment uncertainty.

Equipment List

Description and Model	Last Cal	Serial Number
Helmholtz coil – 60cm	Calibration Not required	AZK
Amplifier- Amplifier Research 200A400	Calibration Not required	N/A
3dB attenuator - Fairview Microwave - SA3N500-03		N/A
Signal Generator -Agilent EXG N51718	Calibration Not required	MY53050502
Isotropic E/H field Probe – SMP2/WP400	4 DEC 2022	19SN1063/19WP100530
Spectrum Analyzer - E4440A 3Hz-26.5GHz	19 OCT 2022	MY48250777
1cm probe – Beehive 100A	Calibration Not required	1019

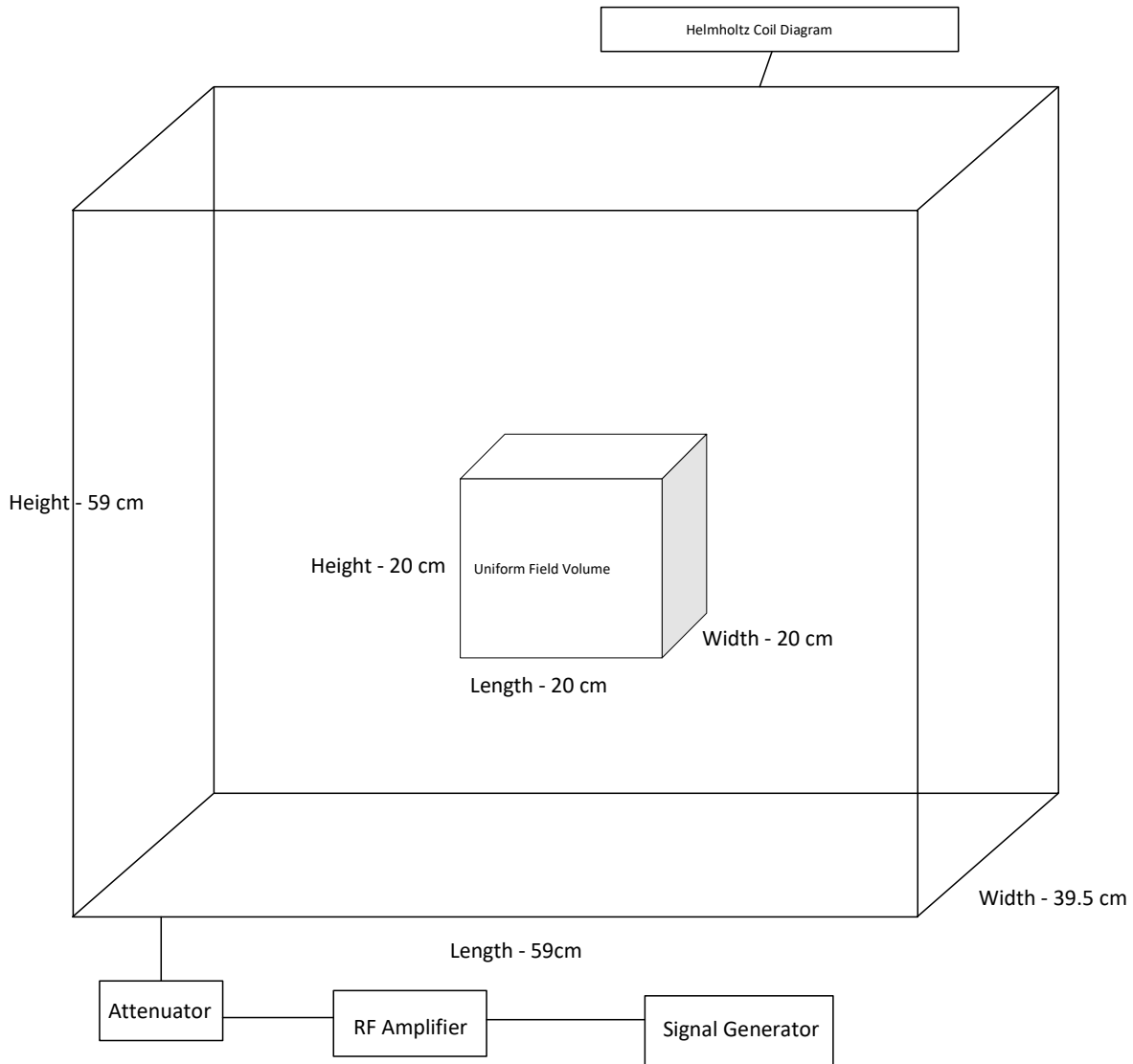


Figure BB Helmholtz Block Diagram

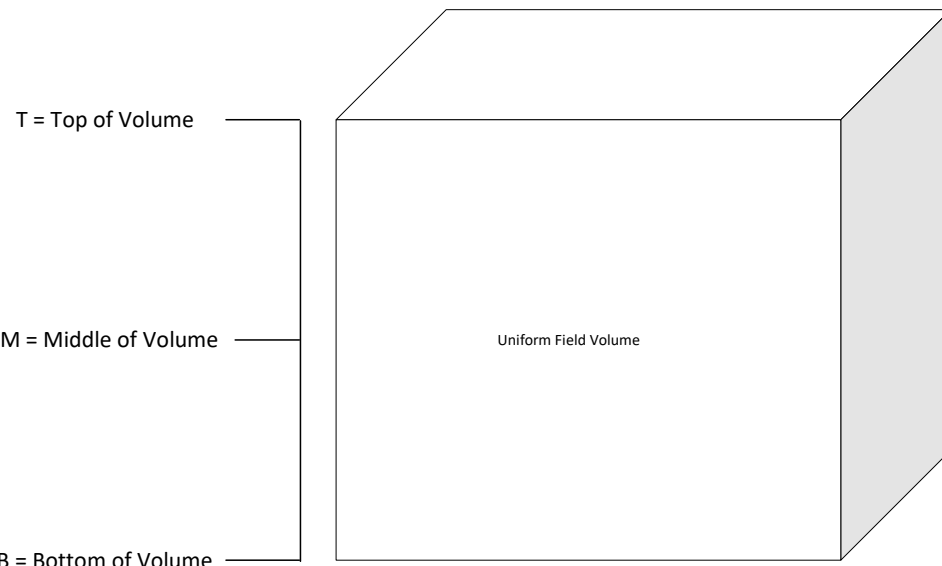
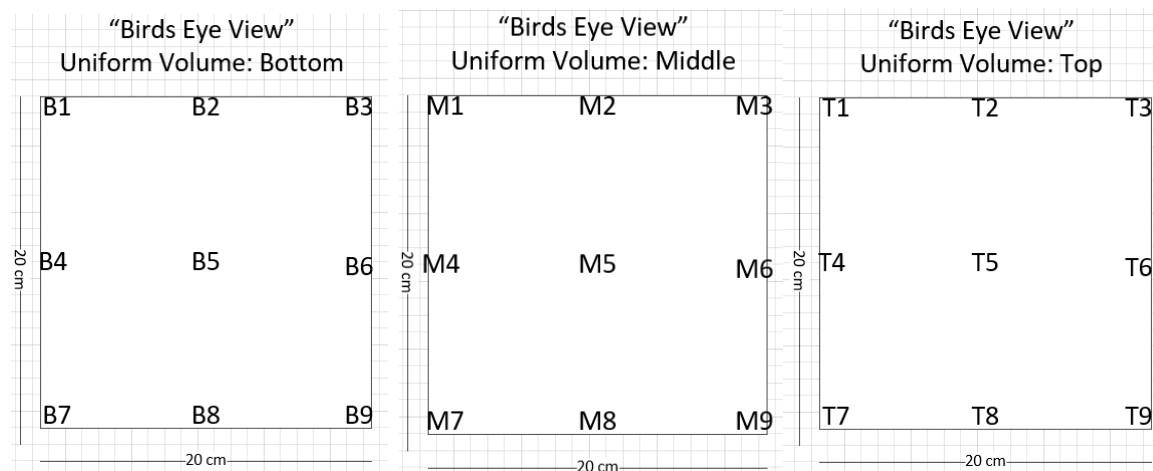


Figure CC Uniform Field Volume Block Diagram



Bottom Location	Bottom Field (A/m)	Middle Location	Middle Field (A/m)	Top Location	Top Field (A/m)
B1	2.1	M1	1.93	T1	1.88
B2	1.81	M2	2.03	T2	1.87
B3	2.02	M3	2.08	T3	2.11
B4	2.06	M4	1.97	T4	2.18
B5	1.84	M5*	2.00	T5	1.96
B6	2.01	M6	2.09	T6	2.13

Bottom Location	Bottom Field (A/m)	Middle Location	Middle Field (A/m)	Top Location	Top Field (A/m)
B7	2.06	M7	1.94	T7	2.17
B8	1.81	M8	2.09	T8	1.9
B9	2.09	M9	2.16	T9	2.17

*Center of volume

Max-pos T4 (A/m)	2.18
Min-pos B8 (A/m)	1.81

Table 2 Uniform Field Measurements

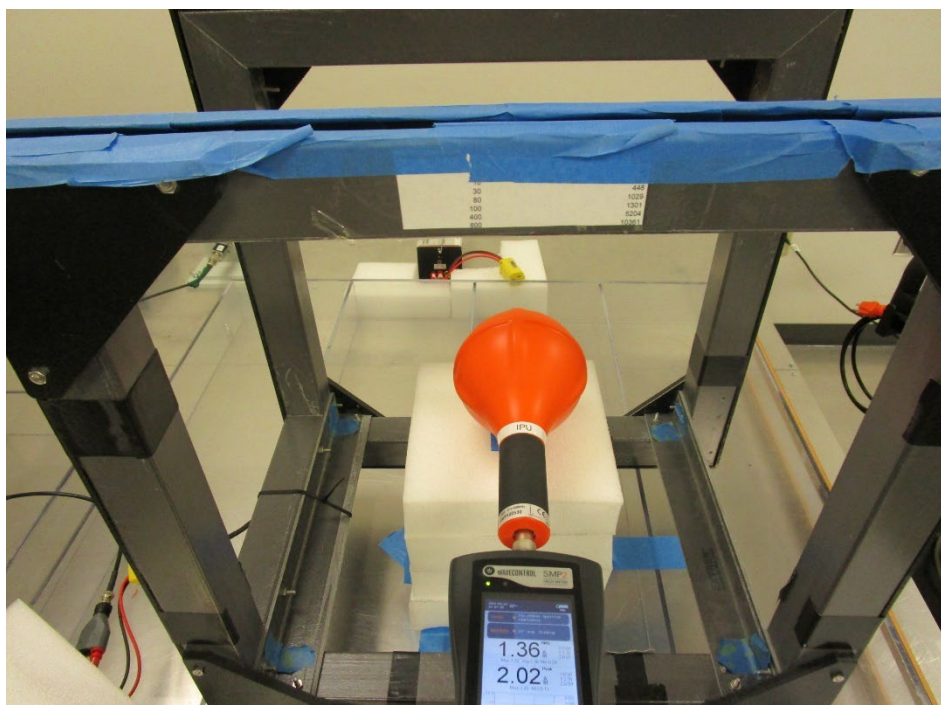


Figure DD Example of Calibrated Probe at Center of Coil

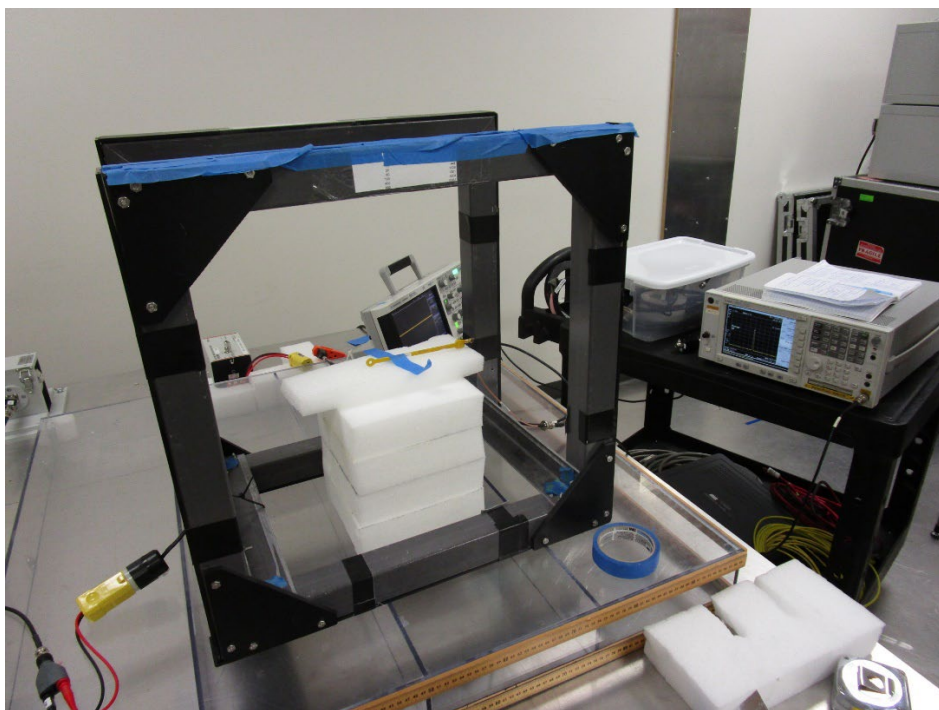


Figure EE Example of 1cm probe at Center of Coil

Measurement Equipment	Value (A/m)
Calibrated Isotropic Probe	1.99
1cm Loop probe	1.80
Percent Error:	9.5%

Figure FF - Probe uncertainty

Measurement Equipment	Value (%)
Calibrated field probe uncertainty:	5
Spectrum analyzer	1.1
RSS:	5.1%

Figure GG - Measurement equipment uncertainty

BeeHive 100A 1cm probe measurements		Dataset		
position	position (inches)	z-axis (dBm)	planar (dBm)	Delta (dB)
pos0	1.64	-48.5	-48.7	0.2
pos1	2.64	-58.1	-58.2	0.1
pos2	3.64	-65.1	-64.9	0.2
RSS:				0.30
				6.7%

Figure HH - Procedure uncertainty

Figure II Comparison of multiple measurements to generate experimental uncertainty.

Uncertainty of the measurement equipment and procedure

Component	Uncertainty (%)
Probe	9.5
Measurement equipment	5.1
Procedure	6.7
RSS:	12.7

Uncertainty of the DUT model

loop probe output power					
d (inches)	num (dBm)	ref (dBm)	$v \propto H_{num} ^2$ (W)	$v \propto H_{ref} ^2$ (W)	U_{SAR}
0.26	-28.4	-28.3	0.00145	0.00148	2%
1.40	-43.8	-45.7	0.00004	0.00003	1.0%
1.64	-46.7	-48.5	0.00002	0.00001	0.5%
$U_{SAR,d}[\%]$					2.2%

Figure JJ DUT model uncertainty, generated by comparing numerical predictions and reference measurements.

Uncertainty of the DUT model

Uncertainty component	Subclause	Uncertainty (%)
Uncertainty of DUT model	7.3.3	2.2%
Uncertainty of Phantom Model	7.3.4	0%
Uncertainty of the measurement equipment and procedure	*	12.7%
Combined std. uncertainty (k=1)		12.9%

*According to manufacturer specification and/or applied methodology.

Figure KK A combination of uncertainties from previous tables to generate aggregate uncertainty.

Model validation Overlay plots (SPR-002 Issue 2, section 8.3.2)

The measurements were taken using a spectrum analyzer. The spectrum analyzer reported the power created by the probe into a 50-ohm load using units of dBm.

The following formulas were used to convert the simulated H-field in A/m to dBm.

$$dBm = 10 \log \left(\frac{V^2}{2R} * 1000 \right)$$

$$V = \omega \mu_0 H A$$

$$\omega = 2\pi f$$

$$A = \pi r^2$$

Where $r = 0.005$ meters and $f = 280\text{kHz}$.

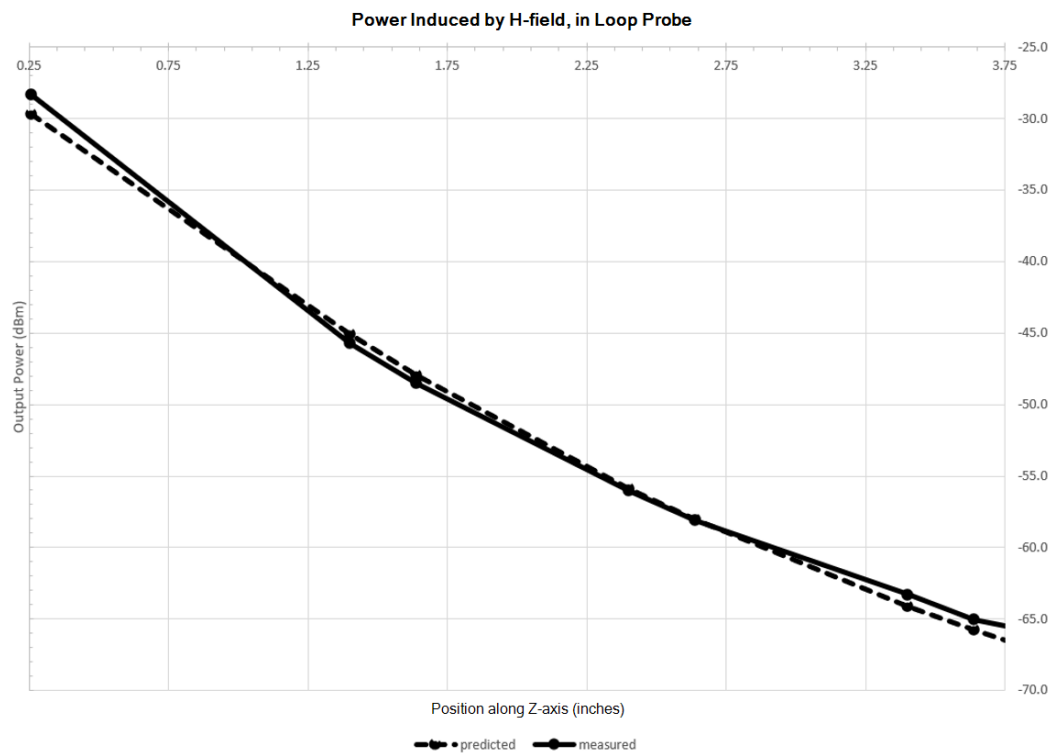


Figure LL Predicted vs. measurement overlays. Z-axis measurements

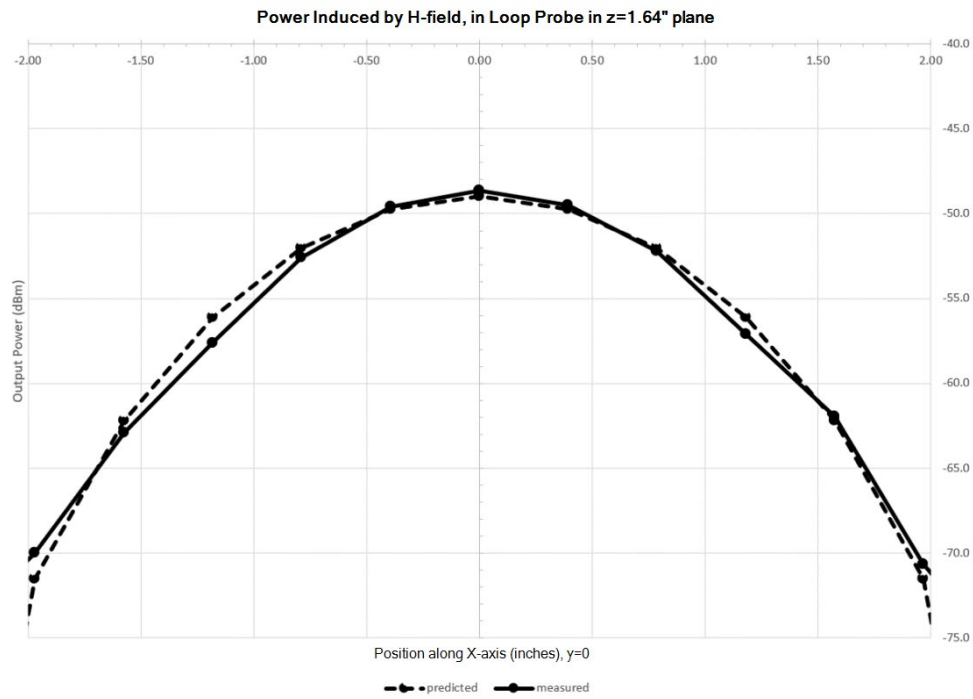


Figure MM Predicted vs. measurement overlays. $z=1.64"$ planar measurement

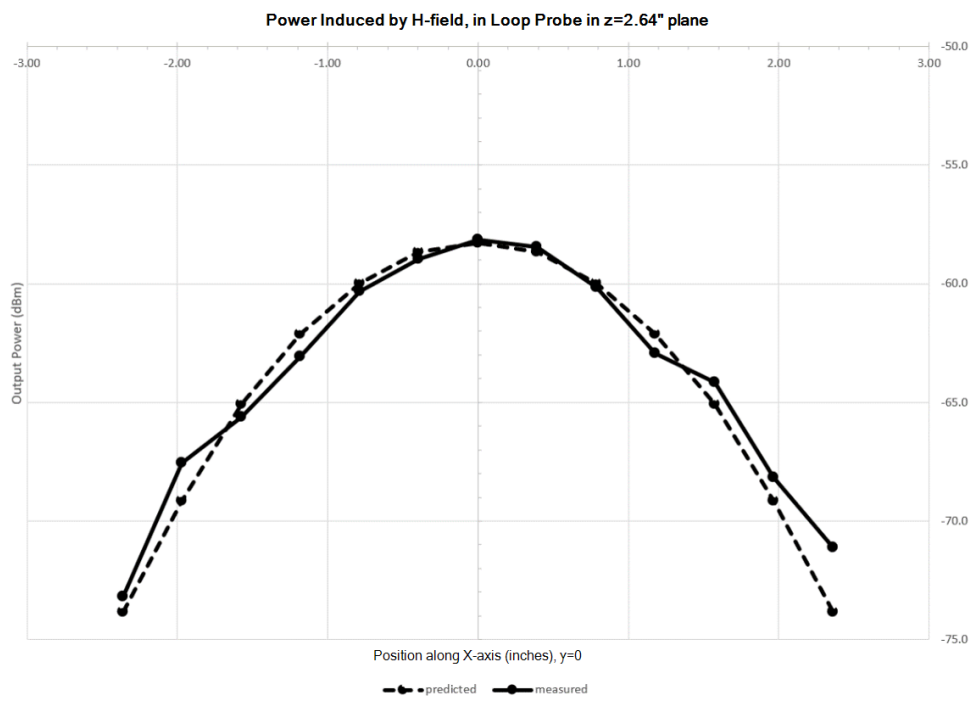


Figure NN Predicted vs. measurement overlays. $z=2.64"$ planar measurement

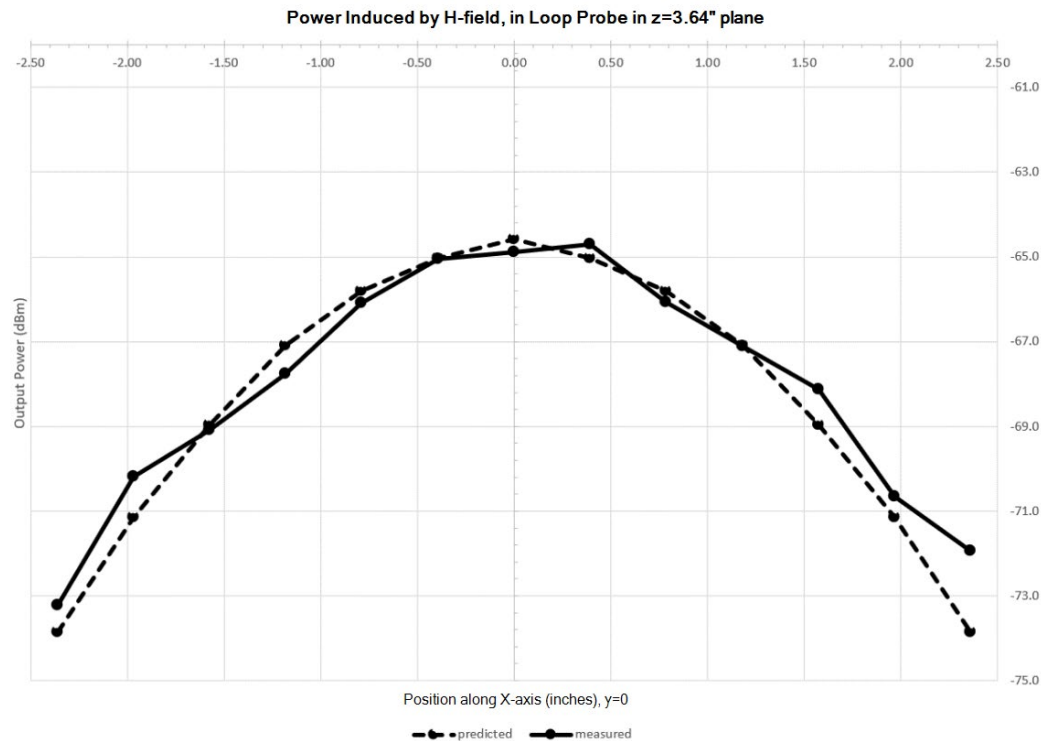


Figure OO Predicted vs. measurement overlays. $z=3.64"$ planar measurement

loop probe output power (dBm)			
	measured/ref	predicted/num	E_n
Axial	-45.7	-45.1	0.51
	-48.5	-48.0	0.44
	-56.0	-55.9	0.12
	-58.1	-58.1	0.01
	-63.3	-64.2	0.85
	-65.1	-65.8	0.73
$Z = 1.64''$ plane	-62.9	-62.2	0.59
	-52.6	-52.0	0.47
	-49.6	-49.7	0.15
	-48.7	-49.0	0.31
	-49.5	-49.7	0.22
	-52.2	-52.0	0.16
	-57.1	-56.1	0.80
	-62.0	-62.2	0.21
	-70.7	-71.5	0.82
$Z = 2.64''$ plane	-60.3	-59.4	0.74
	-59.0	-58.6	0.32
	-58.2	-58.4	0.22
	-58.5	-58.6	0.12
	-60.2	-59.4	0.61
$z = 3.64''$ plane	-66.1	-65.5	0.53
	-65.1	-65.0	0.05
	-64.9	-64.7	0.19
	-64.7	-65.0	0.26
	-66.1	-65.5	0.51
	-67.1	-66.2	0.73
	-68.1	-67.3	0.69

Figure PP Model validation.

Code Verification and Validation

Electromagnetic Solver Software Description

Ansys HFSS uses the Finite Element Method (FEM) to calculate the full 3D electromagnetic field inside a structure. To solve for the electromagnetic fields multiple adaptive passes are performed until the simulation has converged, per the user-defined criteria. An adaptive pass consists of the following:

- Divide the structure into a finite element mesh.
- Compute the modes on each port of the structure.
- Compute the full electromagnetic field pattern inside the structure.
- Compute the generalized S-matrix.
- Check if converged. If not perform another adaptive pass.

The check for convergence occurs after each adaptive pass. To generate the results for this report, nine adaptive passes were performed.

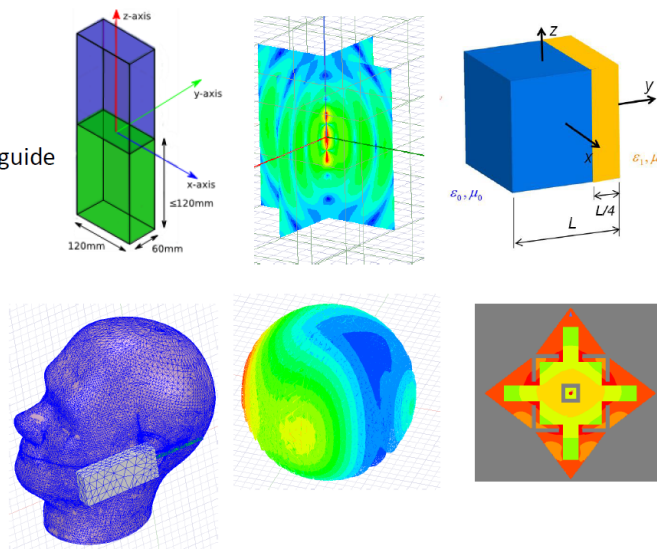
Software Verification

The dipole validation illustrated in the Code Verification and Validation section of this report was calculated using the same software and algorithm as our SAR simulation, as detailed in the preceding section.

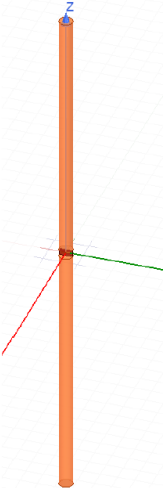
The model used for the SAR calculation was especially modified to have a dense mesh around the coil to accurately account for the small gaps between wires in the coil. The rest of the simulation parameters such as the maximum delta S, max refinements per pass and maximum refinement percentage per pass, were the same as the dipole validation. The model was created in close collaboration with Ansys, the creator of the simulation software.

SAR Code Validation

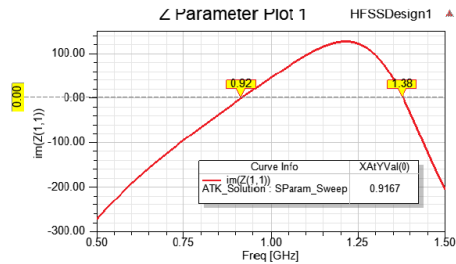
- According to 62704-4:
 - ✓ 8.2.1 → Propagation in a rectangular waveguide
 - ✓ 8.2.3 → Open Boundary condition
 - ✓ 8.3.2 → Weak Patch Free Space
 - ✓ 8.3.3 → Dielectric layered weak patch
 - ✓ 8.4 → SAR Averaging Verification
 - ✓ 8.5.1 → Mie Sphere
 - ✓ 8.5.2 → Generic Dipole
 - ✓ 8.5.3 → Microstrip terminated with ABC
 - ✓ 8.5.4 → SAR calculation SAM
 - ✓ 8.5.5 → Flat Phantom



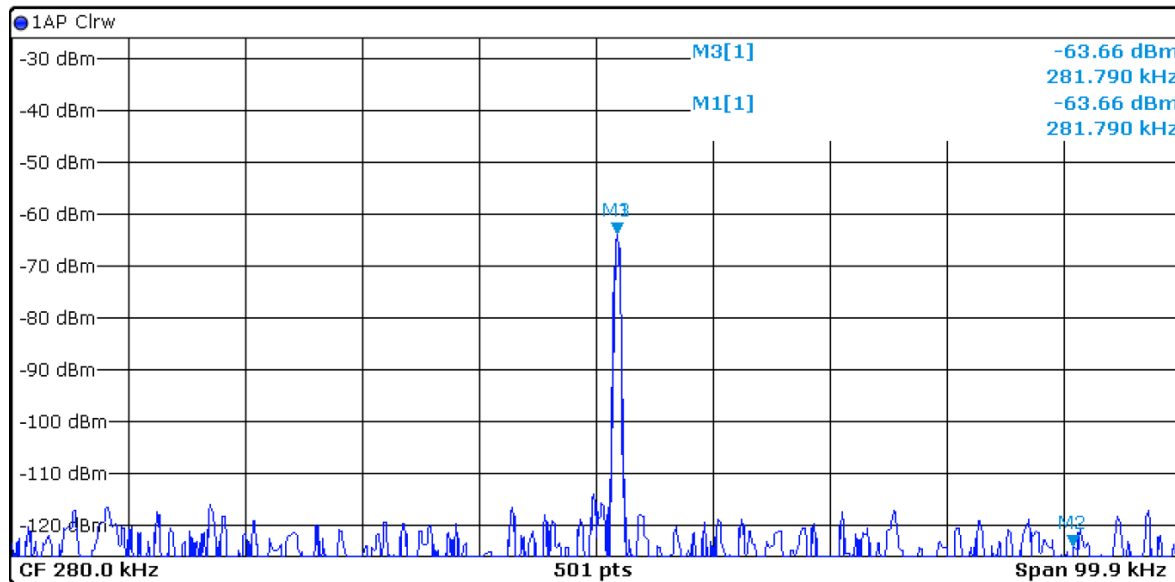
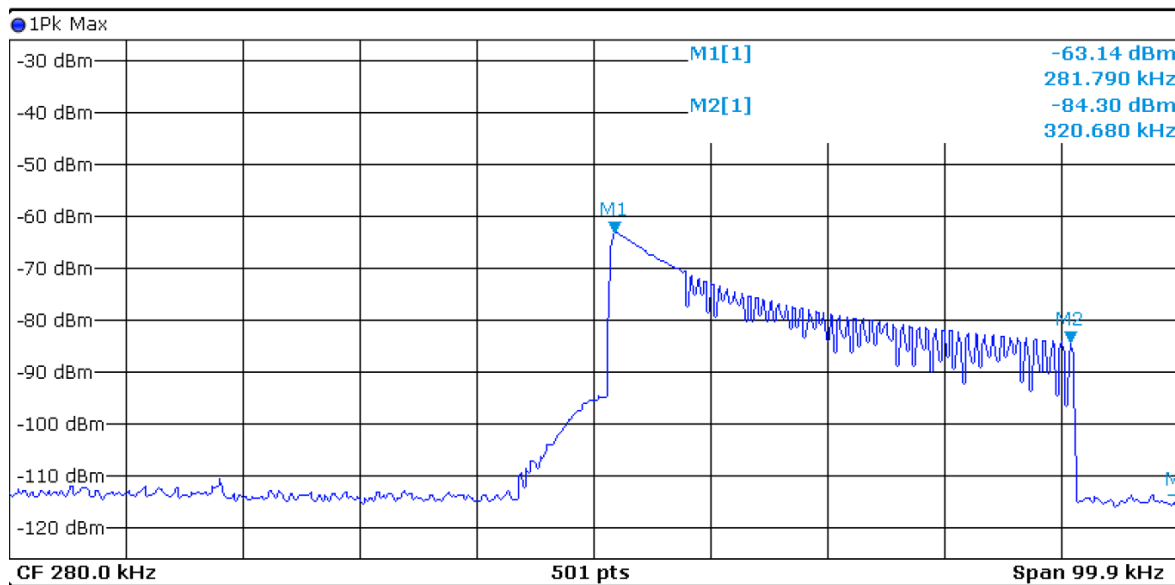
Reference 8.5.2 – Generic Dipole



Quantity	Simulation result	Tolerance
$\text{Re}\{Z\}$ at 0.8 GHz	44.04Ω	$25\Omega < \text{Re}\{Z\} < 50\Omega$
$\text{Im}\{Z\}$ at 0.8 GHz	-65.66Ω	$-100\Omega < \text{Im}\{Z\} < -50\Omega$
$\text{Re}\{Z\}$ at 0.9 GHz	69.2Ω	$50\Omega < \text{Re}\{Z\} < 75\Omega$
$\text{Im}\{Z\}$ at 0.9 GHz	-7.18Ω	$-25\Omega < \text{Im}\{Z\} < 0\Omega$
Frequency for $\text{Im}\{Z\} = 0$	916 MHz	$900\text{ MHz} < f < 950\text{ MHz}$
Maximum power budget error	0.18%	< 5 %



Evaluation Process and Results



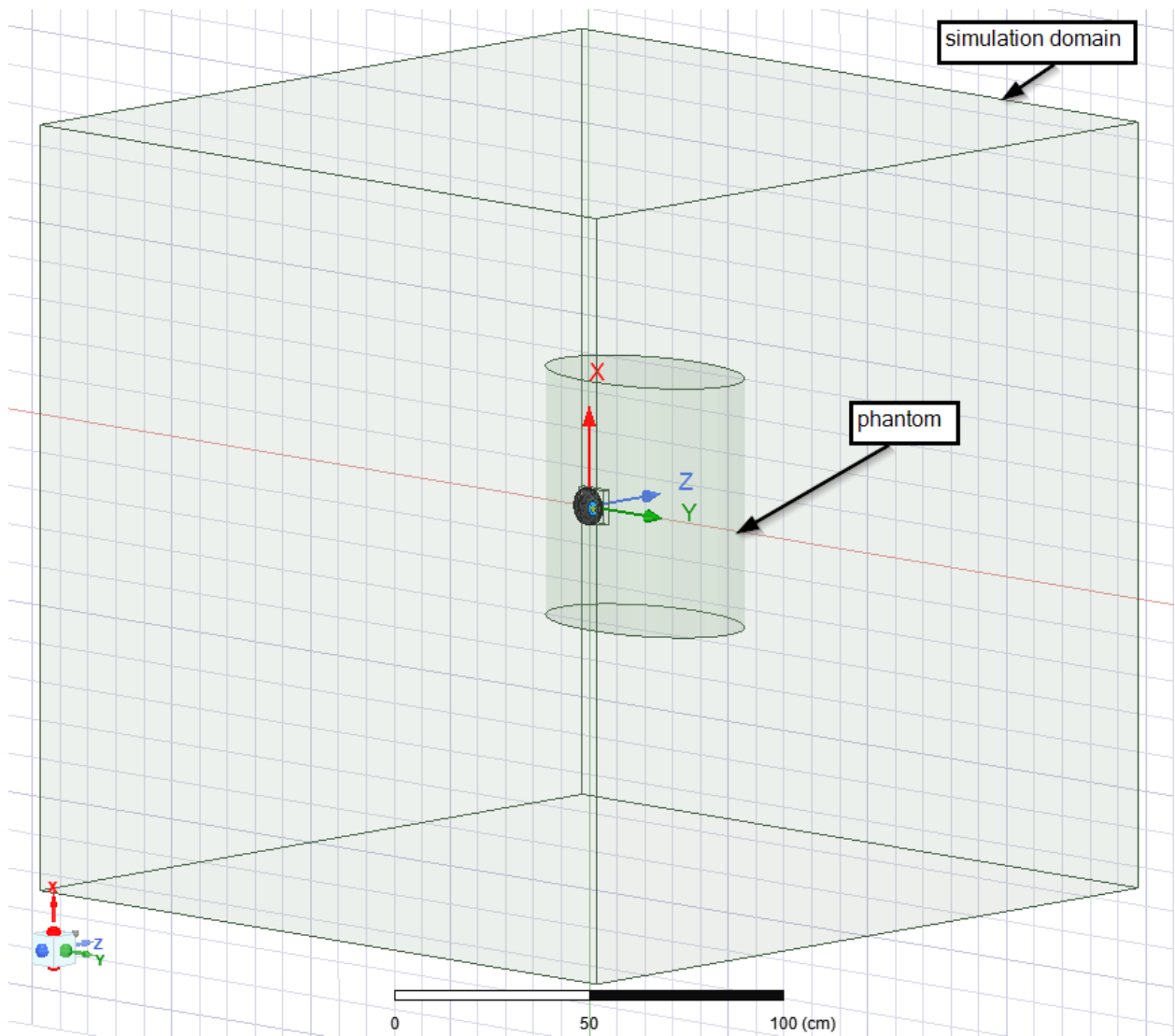


Figure SS Simulation Domain

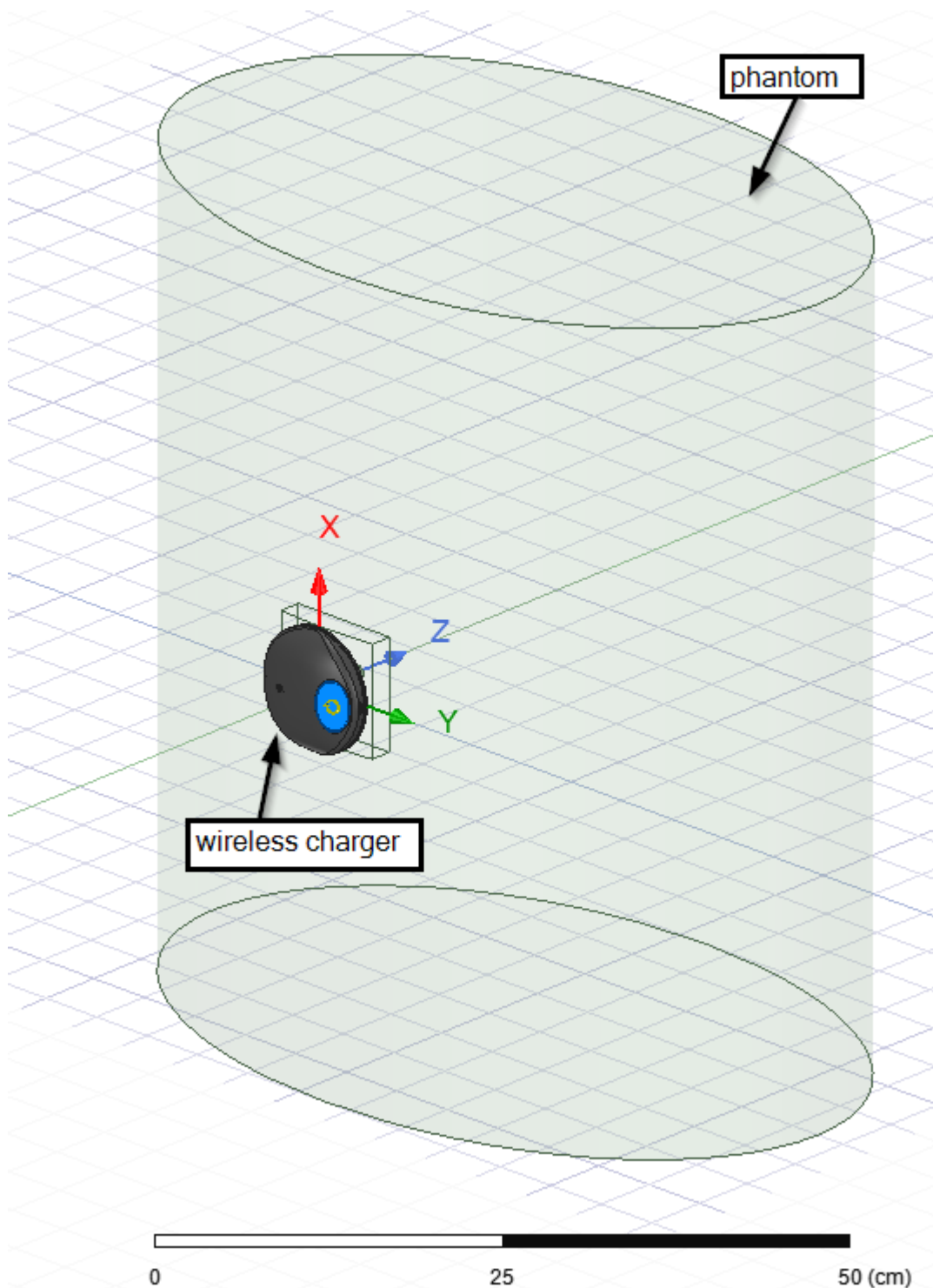


Figure TT Phantom with Charger

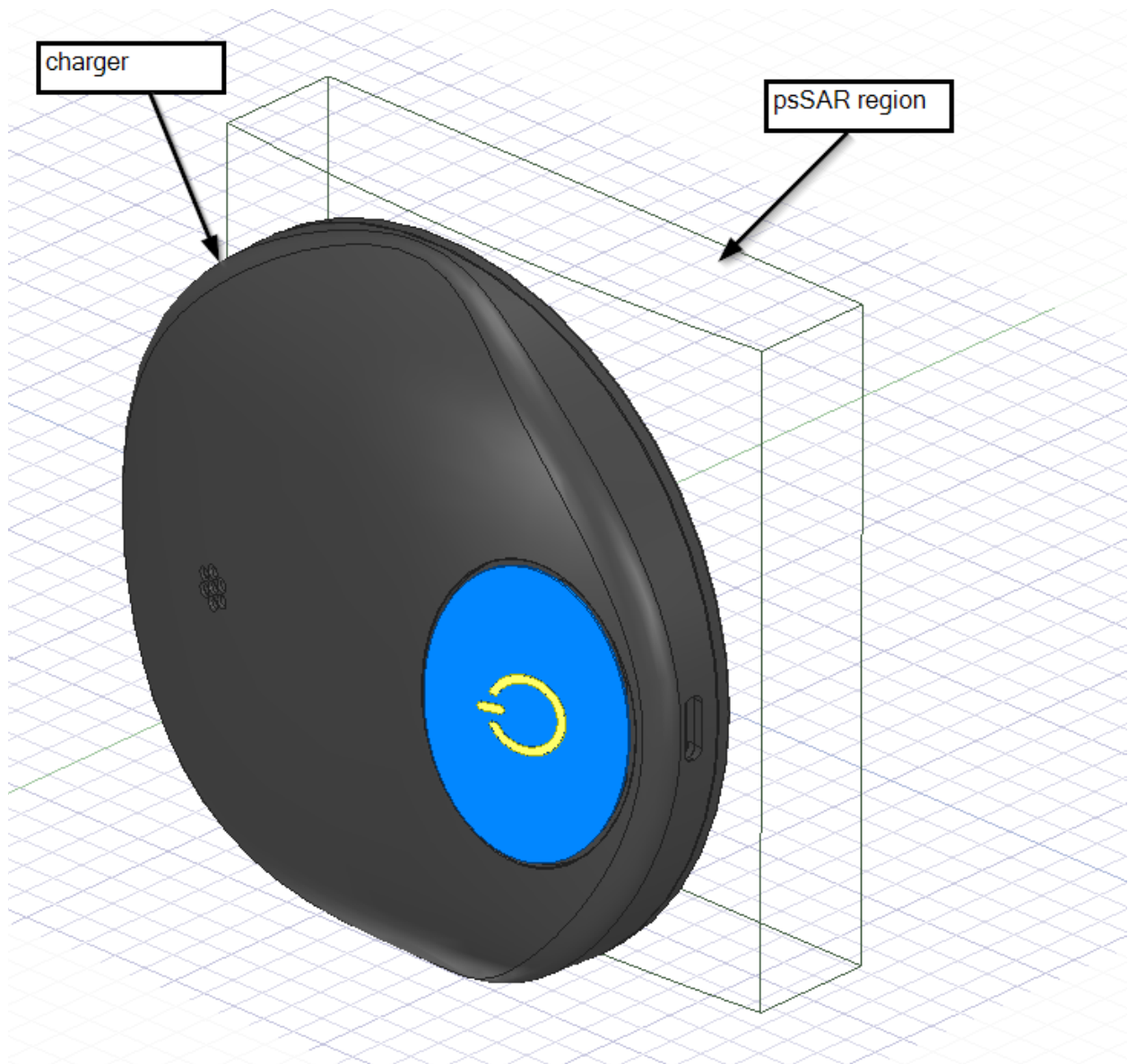


Figure UU psSAR region with Charger

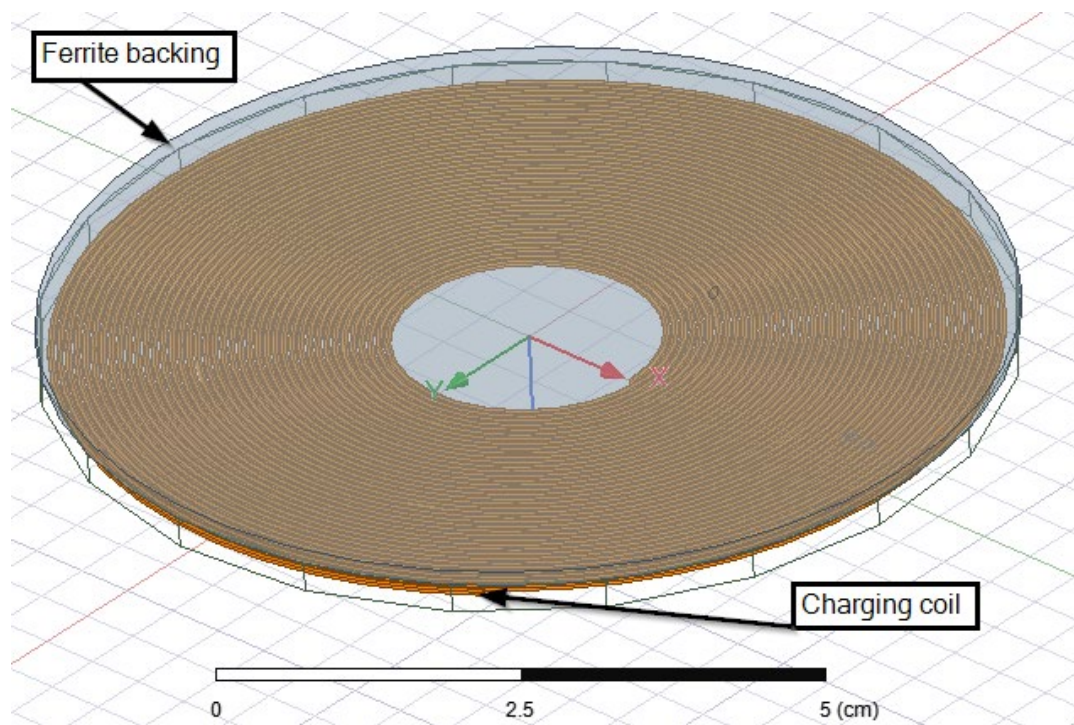


Figure VV Illustration Charger Coil

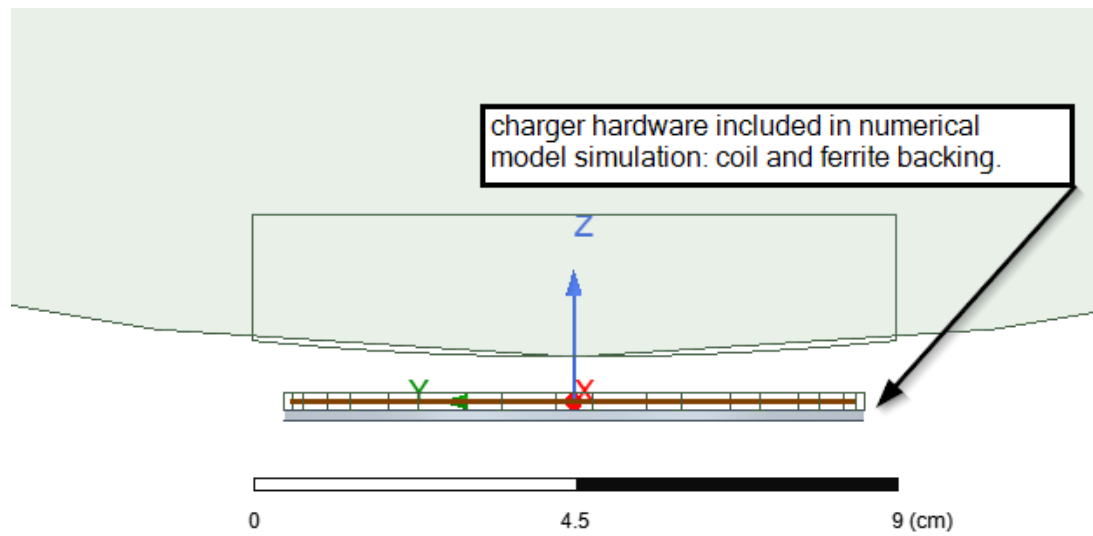


Figure WW Illustration Top View of Coil 0.32 cm from Phantom

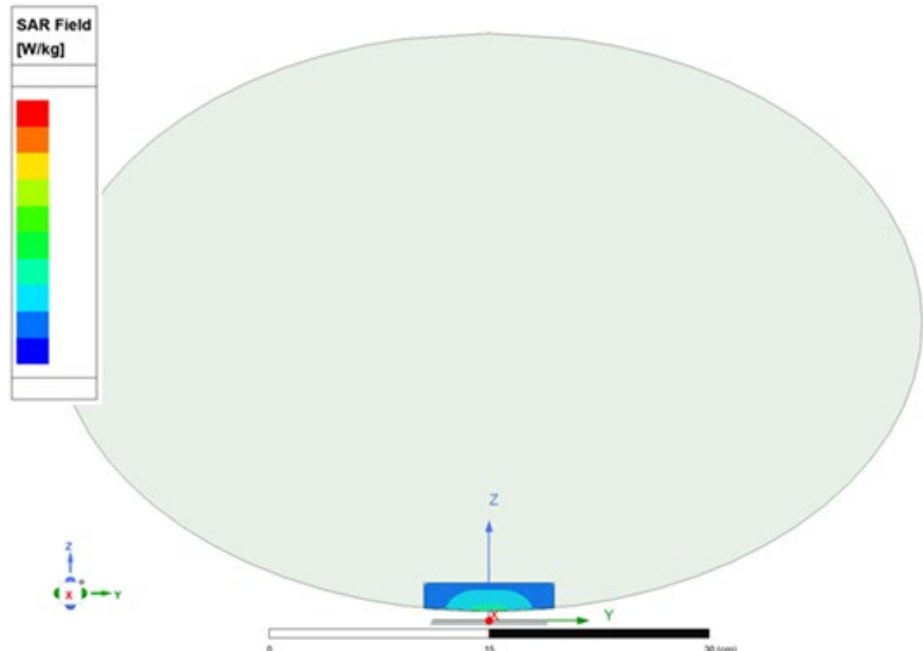


Figure XX Panoramic view of Charger and Phantom

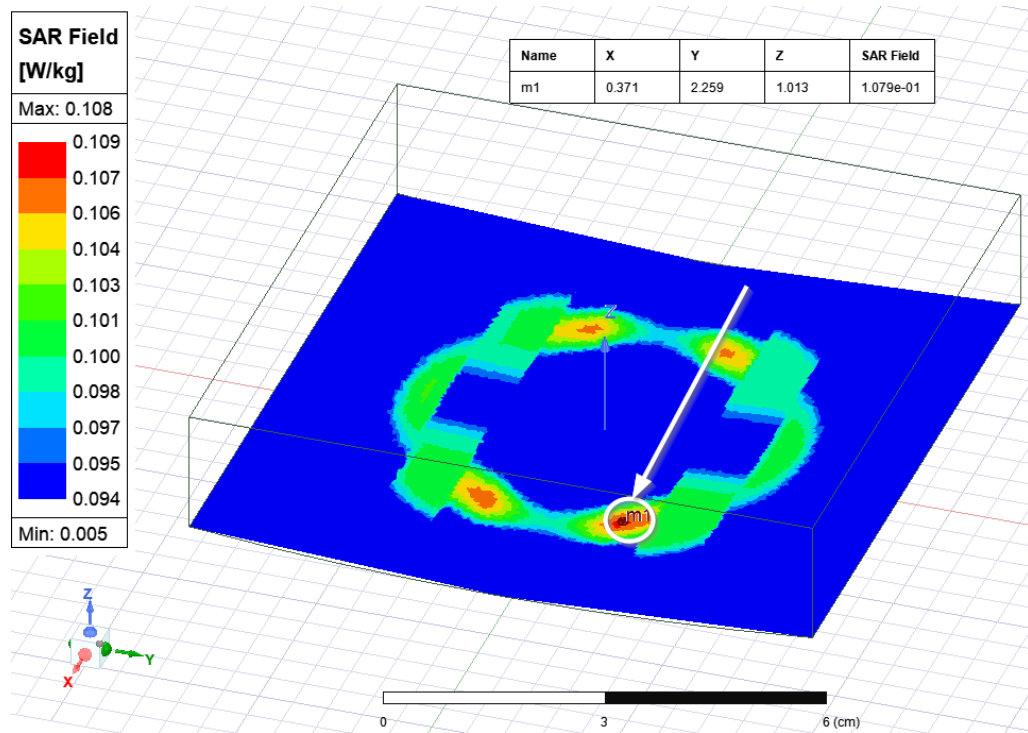


Figure YY Trimetric view with highlighted Maximum Average SAR location over 1gram ((indicated by white arrow))

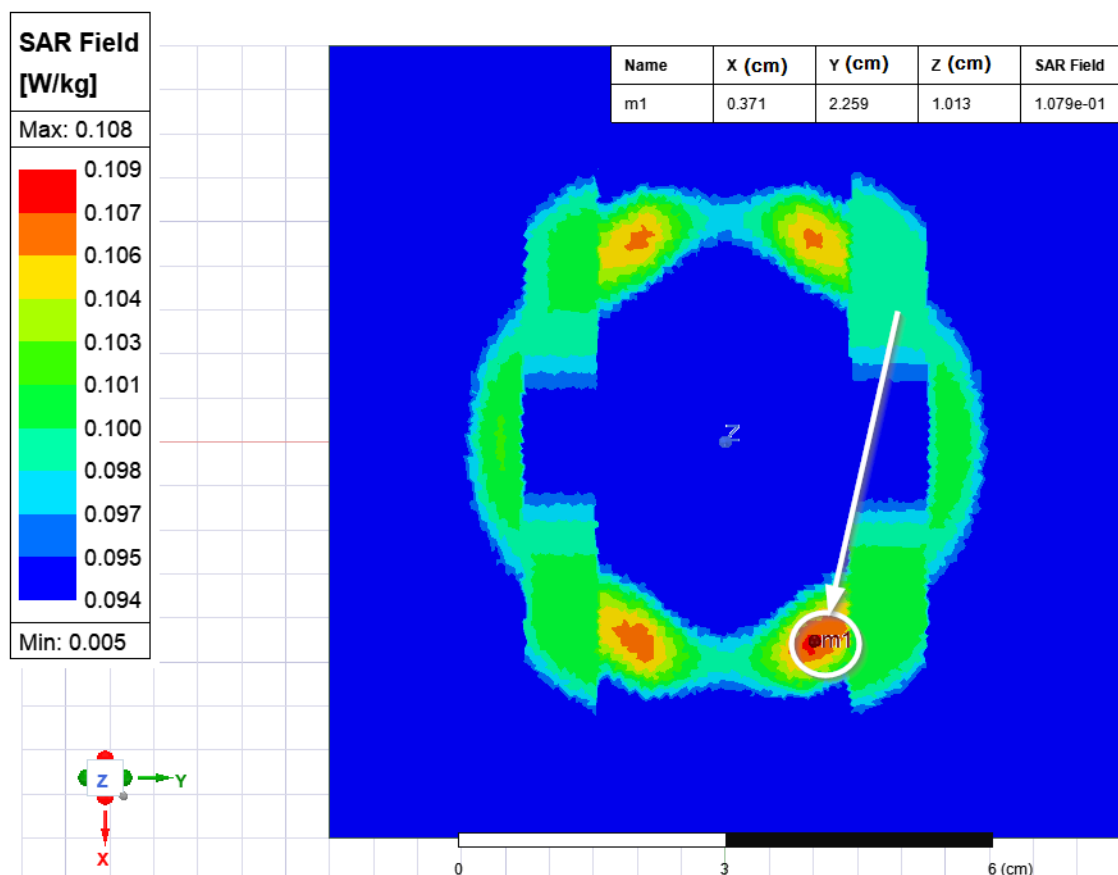


Figure ZZ Top-Down view with highlighted Maximum Average SAR location over 1gram ((indicated by white arrow)

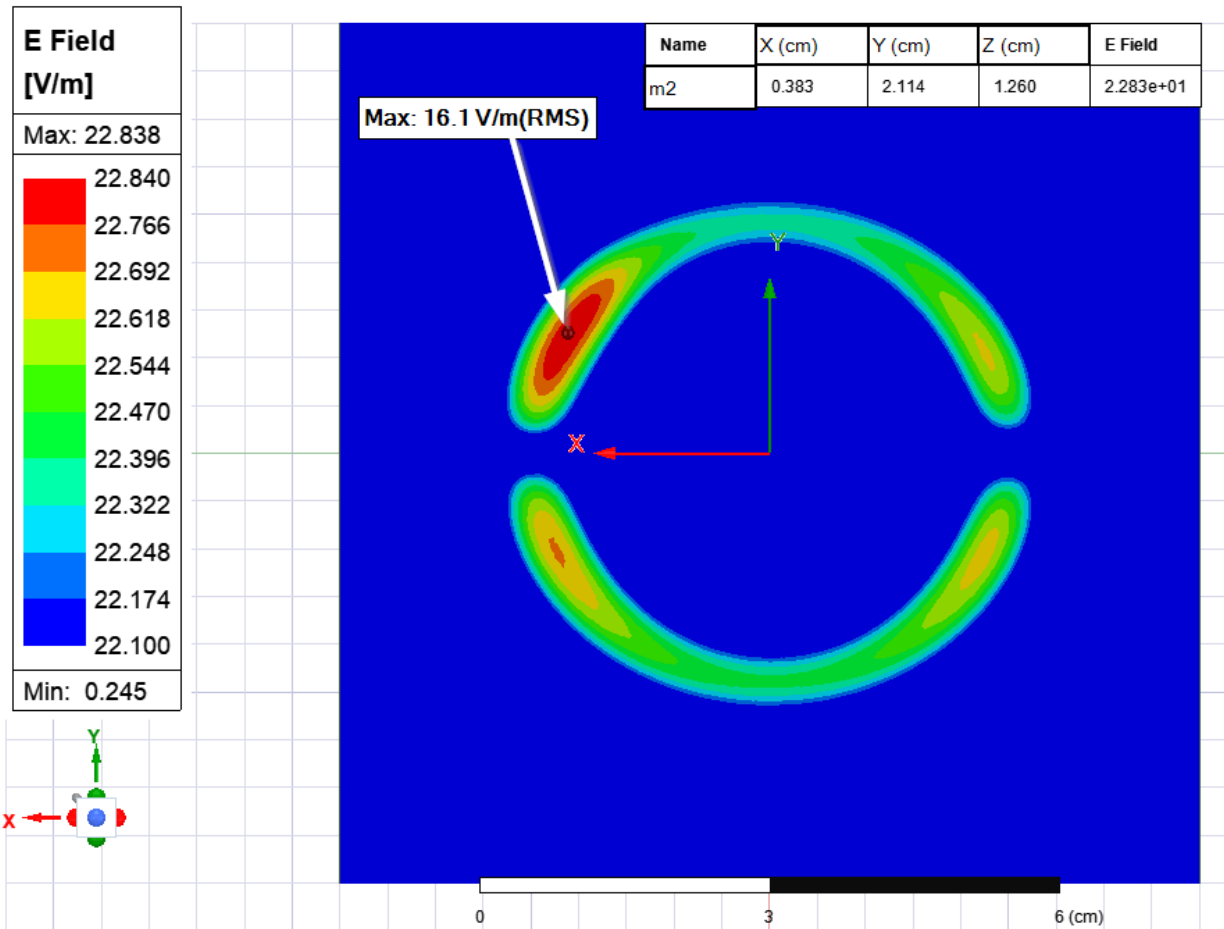


Figure 18 - Location of peak E-field (indicated by white arrow).

SAR									
Radio Operating Range	Transmit Frequency	Duty Cycle	SAR Averaging time	SAR _{BR} (W/kg)	N	SAR (f ₁) (W/kg)	ER _{SAR-BR}	Compliant	Result
WPT 266-320kHz	280kHz	100%	N/A*	1.6	1	0.11	0.07	Yes	Pass
Internal Electric-Field									
Radio Operating Range	Transmit Frequency	Duty Cycle	SAR Averaging time	E _{BR} (fm) (V/m)	M	E _{int} (f _m) (V/m RMS)	-	Compliant	Result
WPT 266-320kHz	280kHz	100%	N/A*	35.9	1	16.1	-	Yes	Pass

Figure AAA Computational SAR and E-Field Results Table

* The SAR simulation is solved in the frequency domain, and therefore the result is steady state in the time domain. The DUT output was set to a constant frequency and output level. The frequency and power level were the worst-case that the DUT can produce. Therefore, the 6-minute time averaged SAR is no different from the 30-minute averaged SAR or longer.



Abbott Laboratories

Neuromodulation

6901 Preston Rd.

Plano, TX 75024

800-727-7846

END OF DOCUMENT